

Report No. IITRI-U6002-55  
(Triannual Report)

DEVELOPMENT OF SPACE-STABLE  
THERMAL-CONTROL COATINGS

National Aeronautics & Space Administration  
George C. Marshall Space Flight Center  
Huntsville, Alabama

IIT RESEARCH INSTITUTE

Report No. IITRI-U6002-55  
(Triannual Report)

DEVELOPMENT OF SPACE-STABLE  
THERMAL-CONTROL COATINGS

March 1 through July 31, 1967

Contract No. NAS8-5379  
Funded under Code 124-09-05-26-04  
IITRI Project U6002

Prepared by

G. A. Zerlaut,  
G. Noble,  
and F. O. Rogers

of

IIT RESEARCH INSTITUTE  
Technology Center  
Chicago, Illinois 60616

to

George C. Marshall Space Flight Center  
National Aeronautics & Space Administration  
Huntsville, Alabama

Copy No. \_\_\_\_\_

September 22, 1967

IIT RESEARCH INSTITUTE

FOREWORD

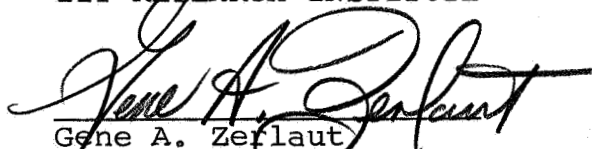
This is Report No. IITRI-U6002-55 (Triannual Report) of IITRI Project U6002, Contract No. NAS8-5379, entitled "Investigation of Environmental Effects on Coatings for Thermal Control of Large Space Vehicles." This report covers the period from March 1 through July 31, 1967. Previous Triannual Reports were issued on October 25, 1963; March 5, 1964; July 20, 1964; December 21, 1964; February 23, 1965; July 20, 1965; November 9, 1965; February 21, 1966; July 11, 1966, November 30, 1966, and February 28, 1967.

Major contributors to the program during this period include Gene A. Zerlaut, project leader, and William C. Courtney, consultation on vacuum problems; Henry DeYoung, coating and specimen formulations; George Kimura, vacuum technology and space simulation tests; Dr. Gordon Noble, solid-state studies on zinc titanate; Frederick O. Rogers, general paint technology and zinc titanate studies; and Samuel Shelfo, reflectance measurements and space simulation tests. Dr. T. H. Meltzer, Assistant Director of Chemistry Research, provided administrative supervision. The work reported herein was performed under the technical direction of the Research Projects Laboratory of the George C. Marshall Space Flight Center; Daniel W. Gates acted as Project Manager.

Prior to March 15, 1966, this contract was funded under Codes 124-09-05-00-14, 933-50-01-00-00, and 908-20-02-01-47.

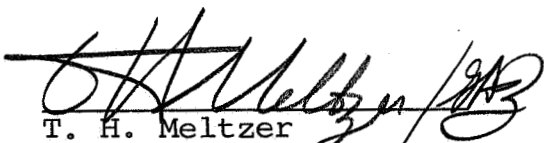
Respectfully submitted,

IIT RESEARCH INSTITUTE



Gene A. Zerlaut  
Senior Chemist-Group Leader  
Polymer Research

Approved by:



T. H. Meltzer  
Assistant Director  
Chemistry Research

GAZ/ms

IIT RESEARCH INSTITUTE

## TABLE OF CONTENTS

|   | Page |
|---|------|
| I. Introduction   | 1    |
| II. The Zinc Titanates                                  | 4    |
| A. Experimental Procedures                              | 6    |
| B. Stability to UV Radiation in Vacuum                  | 13   |
| III. The Solid-State Chemistry of Zinc Titanates        | 38   |
| A. Background Discussion                                | 38   |
| B. Proposed Experiments                                 | 45   |
| IV. Physical Sensitivity of Silicate-Treated Zinc Oxide | 48   |
| V. UV-Vacuum Spectroscopy                               | 56   |
| VI. Summary   | 65   |
| References  | 68   |

### Table

|   |  |    |
|---|--|----|
| 1 | Synthesis Schedule of Zinc Titanates of Different Stoichiometry                                | 7  |
| 2 | Effect of Ultraviolet Irradiation on Several Water-Sprayed Pigment Powders                     | 15 |
| 3 | Effect of 1000 ESH Ultraviolet Irradiation in Vacuum on a Series of Zinc Orthotitanate Powders | 22 |
| 4 | Effect of Ultraviolet Irradiation in Vacuum on Several Zinc Titanates                          | 32 |
| 5 | Effect of Ultraviolet Irradiation in Vacuum on a Series of S-13G Paints                        | 50 |



LIST OF FIGURES

| Figure |  | Page |
|--------|--|------|
| 1      | Reflectance Spectra of Zinc Titanates'<br>Precursors: $\text{ZnO}_2$ , $r\text{-TiO}_2$ and $\alpha\text{-TiO}_2$                  | 8    |
| 2      | Reflectance Spectra of $\text{ZnTiO}_3$ and $\text{Zn}_2\text{Ti}_3\text{O}_8$   | 9    |
| 3      | Reflectance Spectra of Several $\text{Zn}_2\text{TiO}_4$ Powders   | 10   |
| 4      | Effect of UV Irradiation in the IRIF on<br>Cabot's RF-1 Rutile $\text{TiO}_2$  | 16   |
| 5      | Effect of UV Irradiation in the IRIF on<br>Batch A190 $\text{Zn}_2\text{TiO}_4$  | 17   |
| 6      | Effect of Admission of Air on the Reflectance<br>of Batch A-190 $\text{Zn}_2\text{TiO}_4$ (at $0.65 \mu$ )                         | 18   |
| 7      | Effect of UV Irradiation in the IRIF on<br>New Jersey Zinc's A-54-2 $\text{Zn}_2\text{TiO}_4$                                      | 19   |
| 8      | Effect of UV Irradiation in the IRIF on<br>TAM "CP" $\text{ZrO}_2$   | 20   |
| 9      | Effect of UV Irradiation in the IRIF<br>on Batch A111 $\text{Zn}_2\text{TiO}_4$ ( $800^\circ\text{C}/16 \text{ hr}$ )              | 23   |
| 10     | Effect of UV Irradiation in the IRIF on<br>Batch A190 $\text{Zn}_2\text{TiO}_4$ (A111 Extracted with<br>Acetic Acid)               | 24   |
| 11     | Effect of UV Irradiation in the IRIF on<br>Batch A111-N $\text{Zn}_2\text{TiO}_4$ (A111 Extracted with<br>$\text{NH}_4\text{OH}$ ) | 25   |
| 12     | Effect of UV Irradiation in the IRIF on<br>Batch A190-C $\text{Zn}_2\text{TiO}_4$ (A190 + $700^\circ\text{C}/16 \text{ hr}$ )      | 26   |
| 13     | Effect of UV Irradiation in the IRIF on<br>Batch A111-NC $\text{Zn}_2\text{TiO}_4$ (A111-N + $700^\circ\text{C}/16 \text{ hr}$ )   | 27   |
| 14     | Effect of UV Irradiation in the IRIF on<br>Batch A132 $\text{Zn}_2\text{TiO}_4$ ( $1050^\circ\text{C}/16 \text{ hr}$ )             | 28   |

IIT RESEARCH INSTITUTE

LIST OF FIGURES (cont.)

| Figure |   | Page |
|--------|---|------|
| 15     | Effect of UV Irradiation in the IRIF on Batch Al32-A $Zn_2TiO_4$ (Al32 Extracted with Acetic Acid)                | 29   |
| 16     | Effect of UV Irradiation in the IRIF on Batch Al32 $Zn_2TiO_4$ (1050°C/16 hr)                                     | 33   |
| 17     | Effect of UV Irradiation in the IRIF on Batch Al32-A $Zn_2TiO_4$ (Al32 Extracted with Acetic Acid)                | 34   |
| 18     | Effect of UV Irradiation in the IRIF on Batch Al29 $ZnTiO_3$ (850°C/15 hr)  | 35   |
| 19     | Effect of UV Irradiation in the IRIF on Batch Al29-A $ZnTiO_3$ (Al29 Extracted with Acetic Acid)                  | 36   |
| 20     | Effect of UV Irradiation in the IRIF on Batch Al29-AC (Al29-A + 800°C/16 hr)                                      | 37   |
| 21     | Effect of UV Irradiation in the IRIF on a Rutile Opacified Porcelain Enamel                                       | 39   |
| 22     | Effect of UV Irradiation in the IRIF on S-13G Prepared from Sifted Pigment (Paint Grind Time = 3 hr)              | 51   |
| 23     | Effect of UV Irradiation in the IRIF on S-13G Prepared from Unsifted, Unground Pigment (Paint Grind Time = 4 hr)  | 52   |
| 24     | Effect of UV Irradiation in the IRIF on S-13G Prepared from Dry-Ground (30 min) Pigment (Paint Grind Time = 3 hr) | 53   |
| 25     | Effect of UV Irradiation in the IRIF on S-13G Prepared from Hand-mulled Pigment (Paint Grind Time = 3 hr)         | 54   |
| 26     | Effect of UV Irradiation in the IRIF on S-13G Prepared from Remulled Pigment (Paint Grind Time = 5 hr)            | 55   |

LIST OF FIGURES (cont.)

| Figure |  | Page |
|--------|--|------|
| 27     | Schematic of the Dual-Beam Vacuum Chamber  | 59   |
| 28     | The Irradiation and In Situ Measurement Chamber (Sample Mount in Measurement Position)   | 61   |
| 29     | The Irradiation and In Situ Measurement Chamber (Sample Mount in Irradiation Position)   | 62   |
| 30     | Close-up of Irradiation Chamber Showing Rotatable "O" Ring Seal                          | 63   |
| 31     | The Dual-Beam Vacuum Chamber Mated to the B&L Spectronic 505 (Showing Attached Ion Pump) | 64   |

## DEVELOPMENT OF SPACE-STABLE THERMAL-CONTROL COATINGS

### I. INTRODUCTION

The general requirement under this contract is the development of thermal-control surface coatings that possess very low but stable ratios of solar absorptance ( $\alpha_s$ ) to infrared emittance ( $\epsilon_h$ ). Historically this program has been divided into three major phases: (1) inorganic technology, (2) silicone photolysis and silicone paint investigations, and (3) general coatings investigations.

The relative emphasis on each major task has varied during the course of the program according to the urgency of the various problems elucidated by our investigations as well as the availability of both funds and personnel.

Until 1965, zinc oxide (ZnO) was believed to be the most stable white pigment available in terms of the stability of its hemispherical spectral reflectance to ultraviolet irradiation in vacuum (ref. 1-3). However, serious discrepancies in ZnO's behavior were reported between laboratory-simulation data and flight-experiment data obtained from OSO-II (ref. 4) and the Pegasus (ref. 5) materials' experiments.

These data indicated that ZnO-based silicone coatings were considerably less stable than predicted by the extensive space-simulation testing to which they had been subjected. The discrepancy has since been attributed to the formation of an easily bleached (oxygen) infrared absorption band that cannot be observed by classical postexposure reflectance measurements in air. This band was first observed in the laboratory by MacMillan et al (ref. 6) while making in situ measurements of the bidirectional reflectance of ZnO irradiated in vacuum. Confirmation of the bleachable infrared degradation of ZnO first noted by MacMillan et al was reported by Miller (ref. 7) and subsequently by Zerlaut et al (ref. 8,9).

The observations that ZnO exhibits bleachable degradation in the infrared resulted in: (1) the design and construction of a multiple-sample irradiation facility (the IRIF) employing in situ postexposure reflectance measurements (ref. 10), (2) the initiation of inorganic research aimed at securing a satisfactorily stable white pigment, and (3) the design and construction of an evacuated dual-beam, differential ultraviolet spectrometer.

The design of the IRIF was initiated early in 1966, and the facility is now in routine use. A second facility has been constructed and is expected to be in operation by November 1, 1967. The IRIF utilizes an evacuated Edwards-type (ref. 11) integrating sphere for obtaining absolute hemispherical spectral reflectance measurements. This facility was used in the studies reported herein; it is thoroughly discussed in the previous communications and in Ref. 10 and will not be described in this communication.

IIT RESEARCH INSTITUTE

The pigment studies that were initiated as a result of ZnO's behavior involved (1) investigations relating to the stabilization of ZnO against the photodesorption-related infrared degradation observed by the early in situ postexposure measurements and (2) the search for a stable white pigment that does not exhibit significant photodesorption-related damage.

The ZnO stabilization studies involved the treatment of the pigment surface with potassium silicate. (These studies have been supported by the Jet Propulsion Laboratory under contract 951737.) While most of the studies on the development of silicate-treated ZnO paints (S-13G) were performed for the Jet Propulsion Laboratory, studies of the effect of powder reduction (i.e., deagglomeration) on the stability of the silicate-treated ZnO were supported by Contract NAS8-5379 and are reported herein.

The search for a new white pigment has been limited essentially to the zinc titanates.

The work performed during this report period consisted of (1) continued studies of the synthesis, stability to ultraviolet irradiation, and solid-state behavior of zinc titanates, (2) studies of the effect of pregrinding the silicate-treated ZnO prior to manufacture into the S-13G paint, and (3) design, construction, and initial checkout tests on an evacuated, dual-beam vacuum-irradiation-chamber attachment for performing differential ultraviolet spectroscopic measurements in in situ.

## II. THE ZINC TITANATES

The only commercial zinc titanate that has both high reflectance and good stability to ultraviolet irradiation in vacuum was found to be New Jersey Zinc Company's A-54-2, which is chemically designated  $Zn_2TiO_4$ , the orthotitanate. The results of 2000 equivalent sun-hours (ESH) of space-simulation tests on several methyl silicone paints pigmented with A-54-2 were encouraging, and further research was indicated (ref. 12).

An attempt to obtain larger working samples of A-54-2 was unsuccessful, and it became necessary to prepare zinc titanate in our own laboratories.

A search of the literature on zinc titanate revealed at the onset some very interesting conflicts between various researchers. Careful work has been performed by some laboratories, but at the time we commenced work in our own laboratory, complete agreement existed among all sources on only one zinc titanate, the orthotitanate ( $Zn_2TiO_4$ ). The orthotitanate is a spinel that is formed from 2 moles of ZnO and 1 mole of titanium dioxide ( $TiO_2$ ). The reader is referred to the discussion of the pertinent literature in Report No. IITRI-U6002-47 (ref. 12).

A pertinent publication in 1961 by Bartram and Slepetys (ref. 13) to some extent cleared up the discrepancies in the literature. They listed the orthotitanate as most easily prepared from sulfate-process anatase; they stated that a reaction time of 3 hr at from 800 to 1000°C is required. The metatitanate,  $ZnTiO_3$ , they found, required chloride-process rutile  $TiO_2$  and

IIT RESEARCH INSTITUTE

an optimum temperature of 850°C. The solid solution phenomenon claimed by earlier writers appeared to be explained by the claim of Bartram and Slepety's to a third zinc titanate ( $Zn_2Ti_3O_8$ ), the sesquitanate. This is a defect spinel structure made from anatase and ZnO in a ratio of 2 moles ZnO to 3 moles of  $TiO_2$  reacted at a temperature of 700°C for at least 100 hours.

In 1962, Loshkarev in three Soviet papers (ref. 14-16) found only orthotitanate as a compound by using only rutile and ZnO and temperatures up to 1400°C. The reaction between rutile and ZnO did not begin below 740°C.

The existence of unreacted ZnO in the final product, regardless of composition, temperature, or time, was found by Loshkarev and later confirmed at IITRI (ref. 12). Loshkarev reported "very intense shrinkage" (from 15 to 18%) in forming the orthotitanate at temperatures above 1000°C. He therefore recommended slow heating when reaching this temperature. (We followed his advice in our studies; the shrinkage was quite apparent.) The Russian papers do not concede the existence of the metatitanate,  $ZnO \cdot TiO_2$ , nor the sesquitanate listed by Bartram and Slepety's.

The most recent publication on the subject is a Japanese paper by Kubo et al (ref. 17) in which they acknowledge the existence of the three titanates and report success in making the metatitanate of exceptional purity.

In summary, all workers agree on the composition, crystal structure, and characteristics of the orthotitanate; a few agree



upon the existence and structure of the metatitanate; and one only claims the existence and structure of the defect spinel,  $Zn_2Ti_3O_8$ , which we will refer to as the sesquititanate. Although it was considered necessary to first synthesis the orthotitante, the ensuing discussion treats the synthesis of the meta- and sesquititanates first in order to provide a comprehensive review of the reaction between ZnO and  $TiO_2$ .

#### A. Experimental Procedures

The general synthetic procedure, regardless of the specific titanate to be prepared, involved the following general recipe: A distilled-water slurry of the appropriate  $TiO_2$  was adjusted to a pH of 8.5 with  $NH_4OH$  and, along with a distilled-water slurry of ZnO, was agitated for 5 min. The two slurries were combined and agitated together for 15 min. The combined slurry was then vacuum-filtered by using a Büchner funnel. The filter cake was spread on an aluminum sheet and dried at  $100^\circ C$  for 3 hr in a forced-air oven. The material was next dry-ground with a glass muller, packed into a porcelain crucible, and fired at the appropriate temperature for the necessary length of time.

The spectra of all three precursor oxides employed are presented in Figure 1. They are: SP500 ZnO (New Jersey Zinc), RF-1 rutile  $TiO_2$  (Cabot), and TiPure FF anatase  $TiO_2$  (du Pont). These spectra, as well as those presented in Figures 2 and 3, were obtained on our Edwards-type integrating-sphere attachment for the Beckman DK-2A spectroreflectometer. These specimens (and all other zinc titanate specimens whose properties are

IIT RESEARCH INSTITUTE

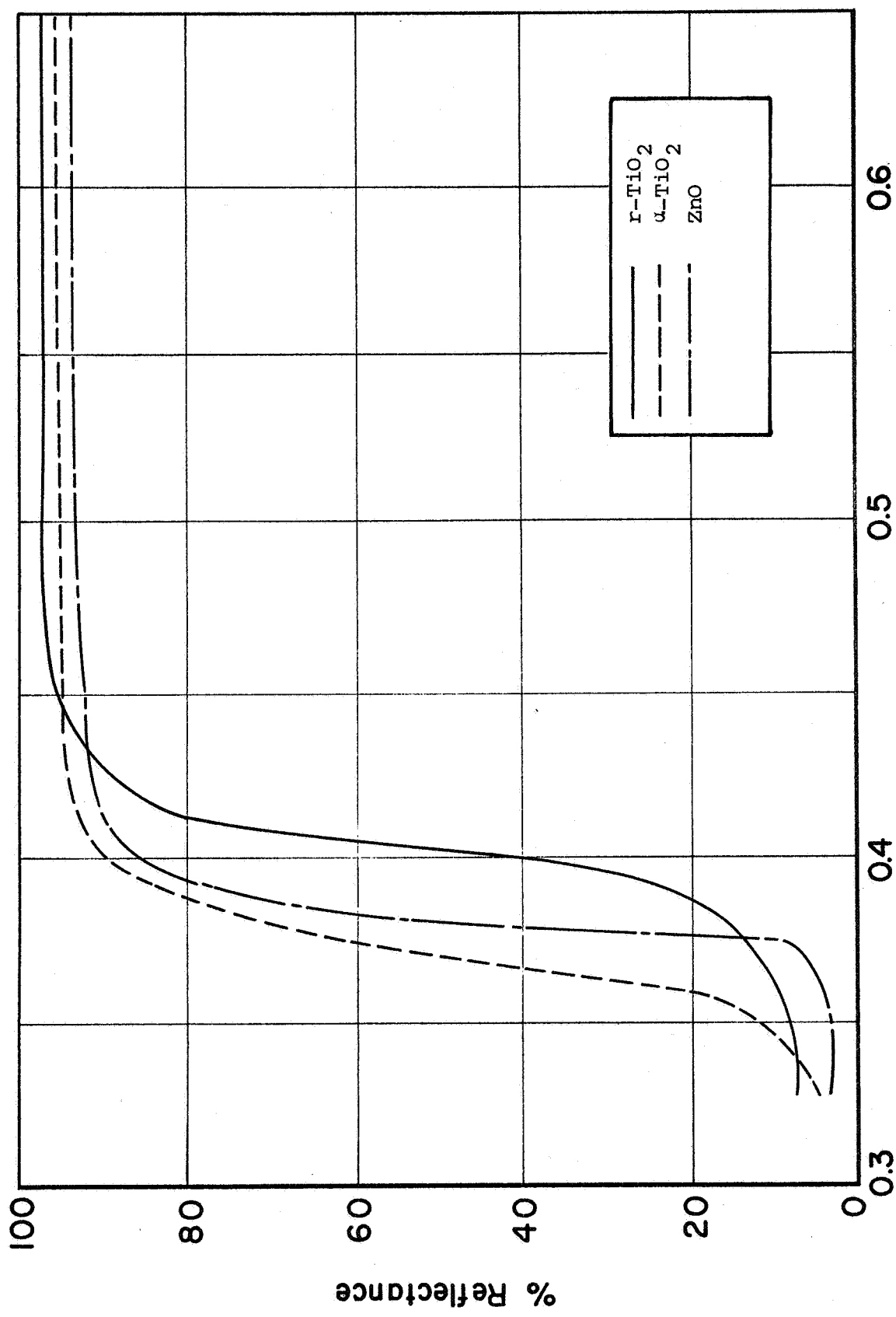
discussed in this report) were prepared by the "wet-spray" technique discussed earlier. The spectra in Figure 1 are presented to provide the necessary background against which the spectra of the synthetic zinc titanates may be evaluated.

The synthesis schedule for the three zinc titanates that were prepared is presented in Table 1. The visible and ultraviolet reflectance spectra of the zinc titanates are presented in Figures 2 and 3. The metatitanate was the yellowist of the three stoichiometries prepared and possessed an absorption edge (Figure 2) similar but considerably more gentle in slope than the rutile from which it was prepared. Like the orthotitanates discussed later, the metatitanate possessed unreacted ZnO, which could be extracted easily with acetic acid (ref. 12). Although the metatitanate possessed only 0.8% excess ZnO, it had profound influence on the absorption spectra, as shown by the broken line in Figure 2.

Table 1

SYNTHESIS SCHEDULE OF ZINC TITANATES OF DIFFERENT STOICHIOMETRY

| ZnO | Mole Ratio<br>of Reactants |                    | Time,<br>hr | Temp.,<br>°C | Structure | Spectra<br>(Fig. No.) |
|-----|----------------------------|--------------------|-------------|--------------|-----------|-----------------------|
|     | a-TiO <sub>2</sub>         | r-TiO <sub>2</sub> |             |              |           |                       |
| 1   | -                          | 1                  | 17          | 850          | Meta      | 2                     |
| 1   | 1                          | -                  | 64          | 700          | Sesqui    | 2                     |
| 2   | 1                          | -                  | 3           | 800          | Ortho     | 3 (A)                 |
| 2   | 1                          | -                  | 16          | 800          | Ortho     | 3 (C)                 |
| 2   | 1                          | -                  | 18          | 1050         | Ortho     | 3 (D)                 |



Wavelength, (μ)

Fig. 1: REFLECTANCE SPECTRA OF ZINC TITANATES' PRECURSORS: ZnO<sub>2</sub>, r-TiO<sub>2</sub> AND α-TiO<sub>2</sub>

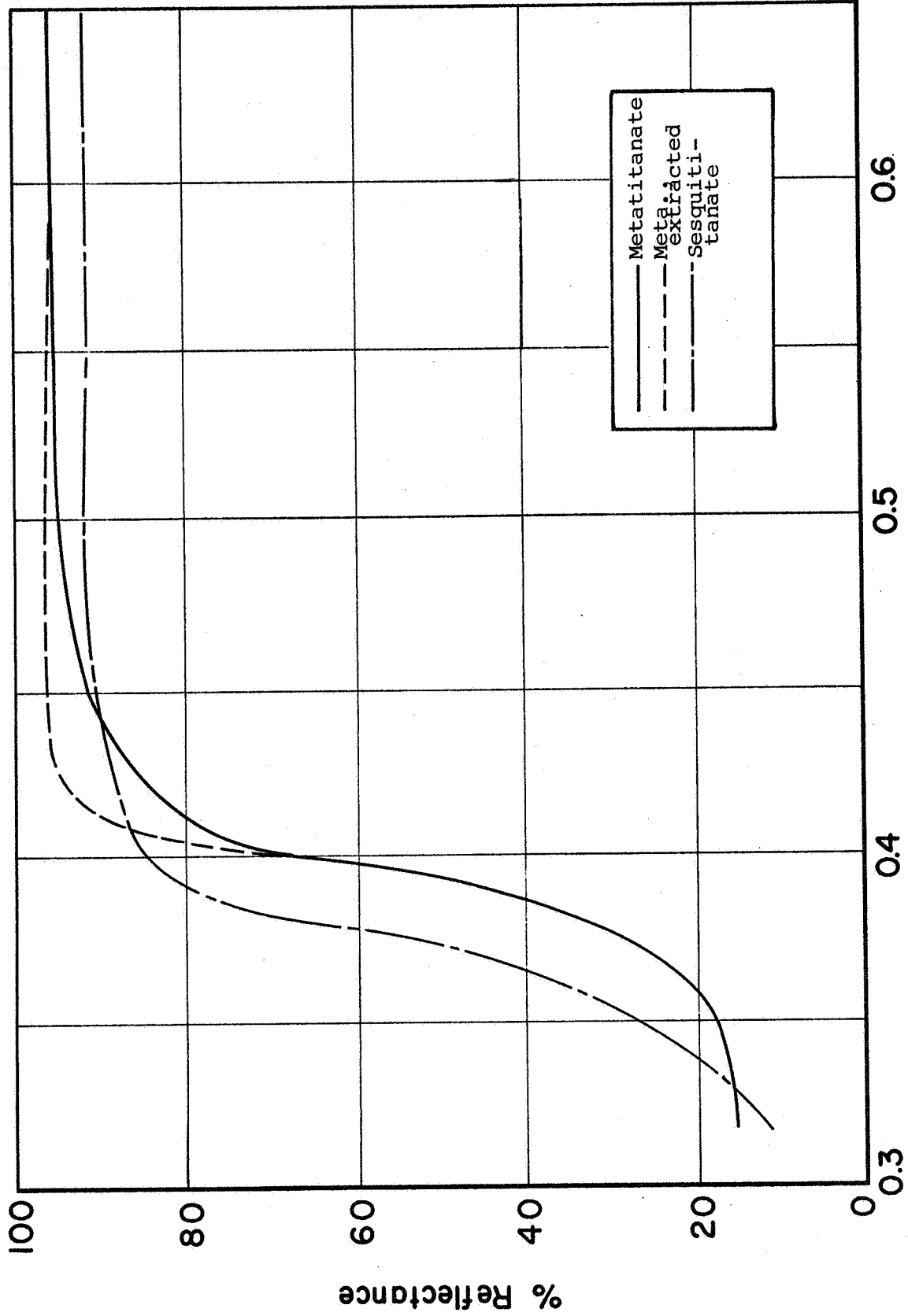


Fig. 2: REFLECTANCE SPECTRA OF  $ZnTiO_3$  AND  $Zn_2Ti_3O_8$

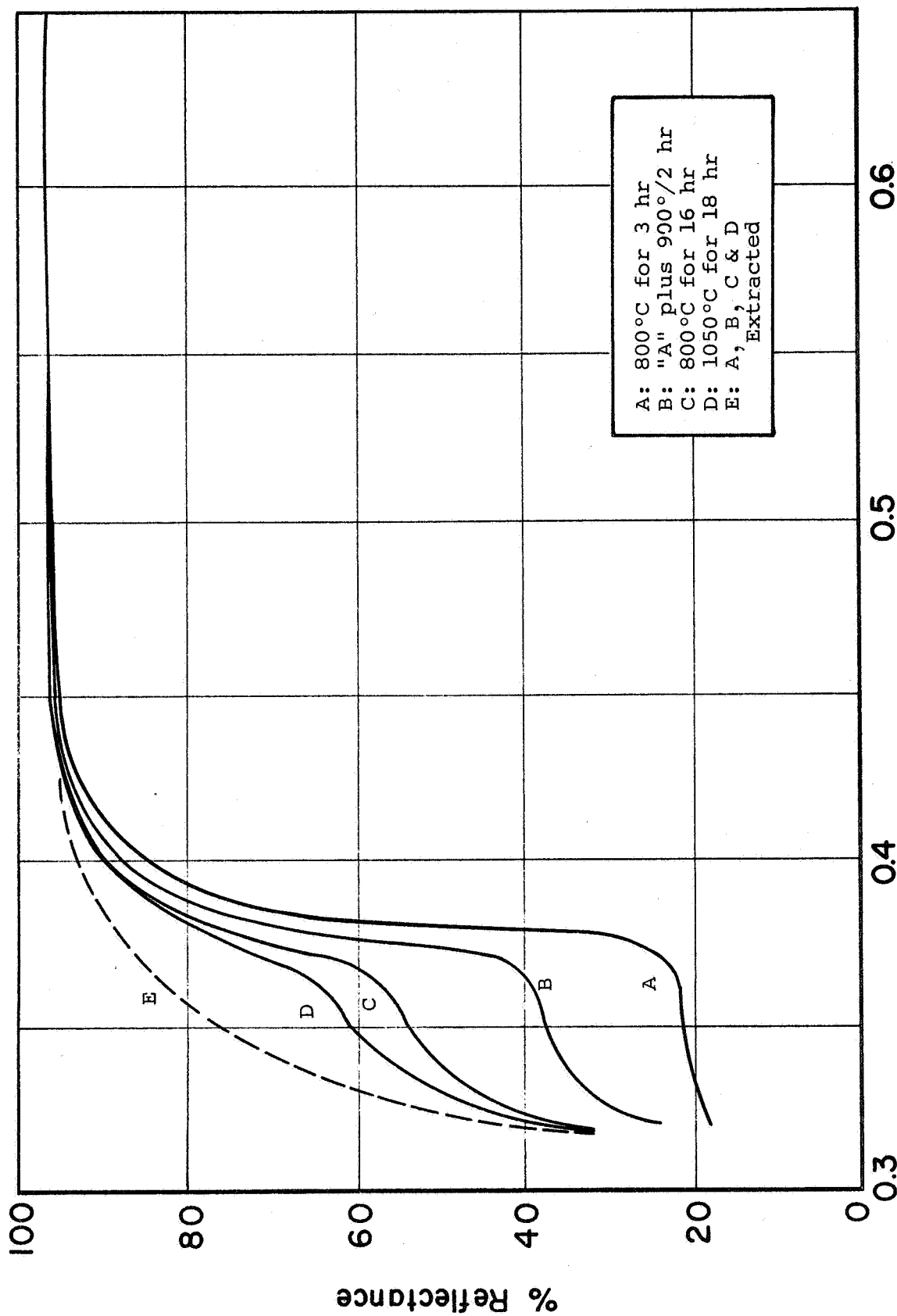


Fig. 3: REFLECTANCE SPECTRA OF SEVERAL  $Zn_2TiO_4$  POWDERS

The sesquitanate was whiter than the unextracted metatitanate but did not, unlike either the meta- or the many orthotitanates that have been examined, exhibit a reflectance increase on extraction of ZnO (Figure 2); the sesquitanate possessed  $\sim 1\%$  excess ZnO. Its absorption edge was not only at a shorter wavelength than either precursor oxide, but it was more gentle in slope than either anatase or ZnO. This structure, which we have termed the sesquitanate, is of a definite stoichiometry since its absorption edge always falls at approximately 3665 A, intermediate between those of the meta- and the orthotitanates. (The absorption edge of the metatitanate is about 4000 A, whereas that of the orthotitanate is 3310 A.)

For reasons that will become apparent, the orthotitanate exhibits the most promise as a thermal-control pigment, and we have therefore addressed our principal efforts to it. The product from the 2:1 mole ratio of ZnO:a-TiO<sub>2</sub> is a very white pigment, brighter to the eye and more reflective than any of the commercial zinc titanates examined. The products of this reaction also appear to be whiter than either of the pigments from which they are prepared.

The reflectance spectra of the orthotitanates (Figure 3) show unmistakably the formation of a compound with a reflectance in the near ultraviolet and short end of the visible spectrum totally unlike any other white pigment previously tested, except for early batches of New Jersey Zinc's A-54-2, which also showed the "step" in the reflectance spectra at about 3500 A.

IIT RESEARCH INSTITUTE

The "step" in the reflectance spectra at 3500 A of all four heats is interpreted as being due to unreacted ZnO, since, in all cases, extraction with acetic acid resulted in a powder that exhibited the spectra presented in curve E of Figure 3. (These spectra require about 2% normalization to 95% reflectance at 6000 A for comparison.)

Batch A (Figure 3) possessed the lowest "step" (20% reflectance) and the highest unreacted ZnO (6%). Recalcination of batch A at 900°C for 2 hr increased the step reflectance to about 38% (5% excess ZnO). Calcination of batch C for 16 hr at 800°C resulted in a significant increase in the reflectance at 3500 A; the increase in reflectance of 55% corresponded to 3% excess ZnO.

Batch D (Figure 3), calcined for 18 hr at 1050°C, exhibited very slight, extractable yellowing and extreme hardness. The fact that residual ZnO still existed (2%), even after additional heating, confirms the work of Loshkarev (ref. 14-16). However, the Russian papers list the hardness as 5 mho; our own impression is that the high-temperature product possesses a hardness of 6 mho.

In summary, the metatitanate,  $ZnTiO_3$ , must be prepared from rutile  $TiO_2$ , preferably of the chloride type. The reaction temperature should be between 800 and 950°C; the reaction is preferably carried out at 850°C. The metatitanate possesses an ilmenite crystal structure and requires a rutile: ZnO mole ratio of 1:1 for preparation.

The sesquitanate,  $Zn_2Ti_3O_8$ , also requires a mole ratio of 1:1 but is prepared from anatase at temperatures in the 700 to 800°C range. It is a defect spinel crystal that, like the metatitanate, transforms to the orthotitanate at temperatures in excess of 950°C.

The orthotitanate,  $Zn_2TiO_4$ , by far the hardest and most reflective of the zinc titanates, must be prepared at a 2:1 mole ratio  $ZnO:TiO_2$  at temperatures above 950°C for maximum conversion of ZnO. The orthotitanate is a spinel-type crystal that will scratch glass.

X-ray diffraction patterns have shown no evidence of intermediate solid solutions of zinc titanates.

#### B. Stability to Ultraviolet Radiation in Vacuum

The stability of  $Zn_2TiO_4$  was at first reported by us (ref. 18) to be excellent after 200 ESH of ultraviolet irradiation; the material examined was prepared at 800°C for 3 hours. However, subsequent space-simulation tests on  $Zn_2TiO_4$  have, for the most part, resulted in severe degradation.

The following discussion deals with the results of three space-simulation tests employing the IRIF -- IRIF tests 5,7, and 12. The results of these tests are presented in Figures 4 through 21, which show the absolute hemispherical spectral reflectance as a function of 2% equal-energy increments. The spectral region 4000 to 7000 Å (visible), where nearly 50% of the solar energy lies, is more significantly and more accurately represented by graphical presentation of data in this manner.

IIT RESEARCH INSTITUTE



## 1. IRIF Test 5

The space-simulation test designated IRIF test 5 was the first space-simulation test to result in severe degradation of  $Zn_2TiO_4$ . Four pigment powder specimens were irradiated for 125 and 600 ESH of ultraviolet radiation in vacuum at a nominal solar intensity of 6X. The powders that were examined in this test included Cabot's Flame Process rutile  $TiO_2$ , an experimental zinc orthotitanate (batch A190) prepared at 800°C for 16 hr, New Jersey Zinc's A-54-2 zinc orthotitanate, and a control specimen of TAM's "CP" zirconium dioxide ( $ZrO_2$ ). (Eight other specimens irradiated in test 5 were prorated costwise to the Jet Propulsion Laboratory on Contract 950746.)

The solar absorptance changes exhibited by the four powders are presented in Table 2. The corresponding reflectance spectra are presented in Figures 4 through 8.

Examination of the data show that the rutile specimen is considerably more stable than  $ZrO_2$  and that the damage, which amounted to a  $\Delta\%_s$  of 0.056, was bleached by about 43% on admission of air.

Figure 5 presents the damage spectra of IITRI's  $Zn_2TiO_4$  batch A190. This specimen was prepared from batch A111 pigment, which possessed residual ZnO that was manifested in a reflectance "step" at 3750 Å. The residual ZnO was extracted with acetic acid. The surprising result of this test was the severe and almost totally bleachable visible-region degradation. The degradation amounted to nearly a 15% decrease in reflectance at 6700 Å, the approximate peak of the damage spectrum.

IIT RESEARCH INSTITUTE

Table 2  
 EFFECT OF ULTRAVIOLET IRRADIATION  
 ON SEVERAL WATER-SPRAYED PIGMENT POWDERS  
 (IRIF Test 5; Solar Intensity 6X)

| Specimen | Material   | Exposure,<br>ESH | Solar Absorptance |            |            |                  |
|----------|--|------------------|-------------------|------------|------------|------------------|
|          |  |                  | $\alpha_1$        | $\alpha_2$ | $\alpha_s$ | $\Delta\alpha_s$ |
| -        | r-TiO <sub>2</sub> (Cabot)                       | 0                | .084              | .042       | .126       | -                |
|          |  | 125              | .100              | .050       | .150       | .024             |
|          |  | 600              | .124              | .058       | .182       | .056             |
|          |  | Air              | .110              | .048       | .158       | .032             |
| S-3-9    | Zn <sub>2</sub> TiO <sub>4</sub> (A-190)         | 0                | .058              | .023       | .081       | -                |
|          |  | 600              | .117              | .057       | .174       | .093             |
|          |  | Air              | .062              | .034       | .096       | .015             |
| S-3-10   | Zn <sub>2</sub> TiO <sub>4</sub><br>(NJZ A-54-2) | 0                | .077              | .036       | .113       | -                |
|          |  | 600              | .120              | .076       | .196       | .083             |
|          |  | Air              | .094              | .045       | .139       | .026             |
| -        | ZrO <sub>2</sub>                                 | 0                | .064              | .073       | .137       | -                |
|          |  | 125              | .112              | .074       | .186       | .049             |
|          |  | 600              | .184              | .085       | .269       | .132             |
|          |  | Air              | .161              | .078       | .239       | .102             |

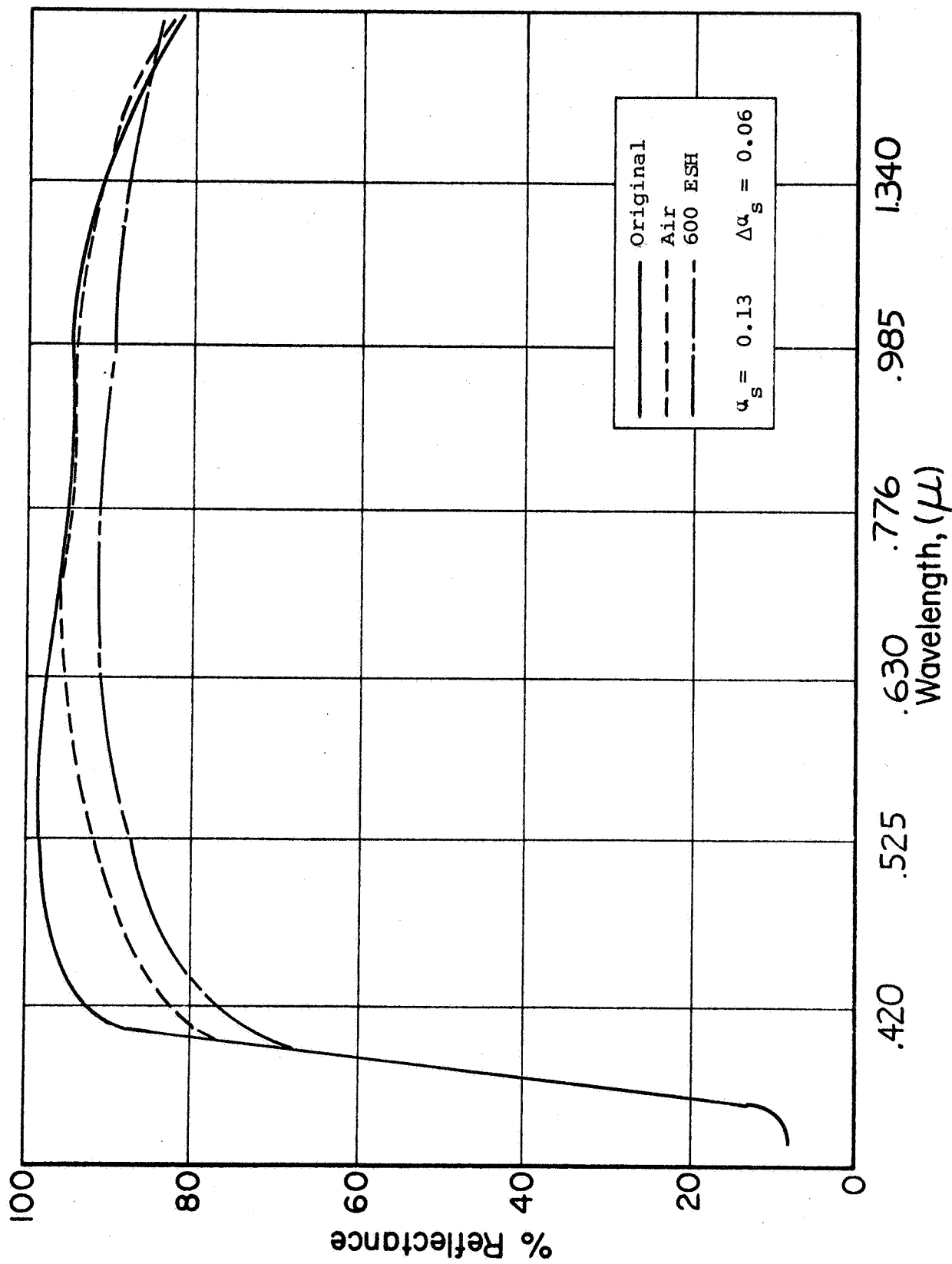


Fig. 4: EFFECT OF UV IRRADIATION IN THE IRIF ON CABOT'S RF-1 RUTILE TiO<sub>2</sub>

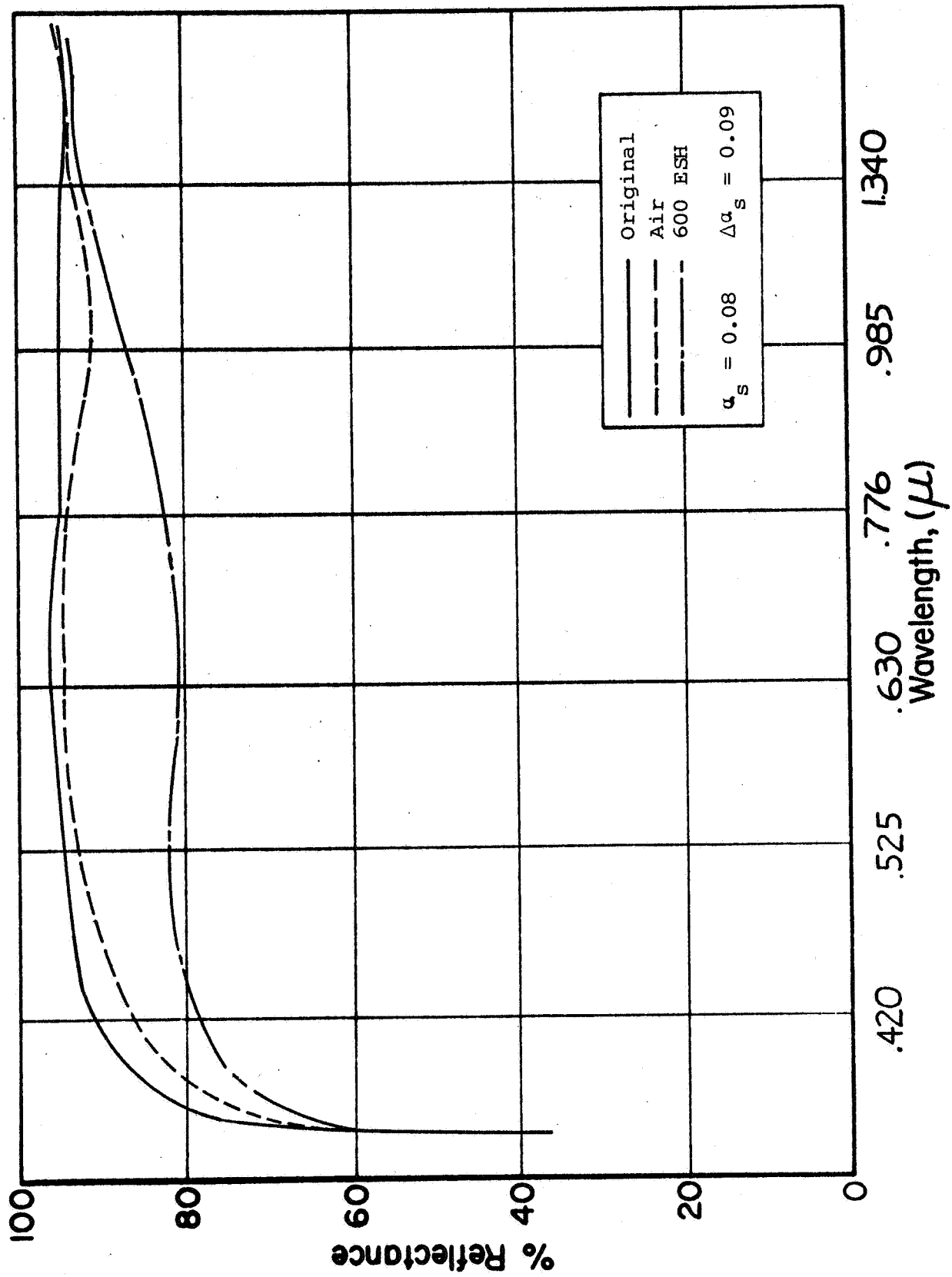
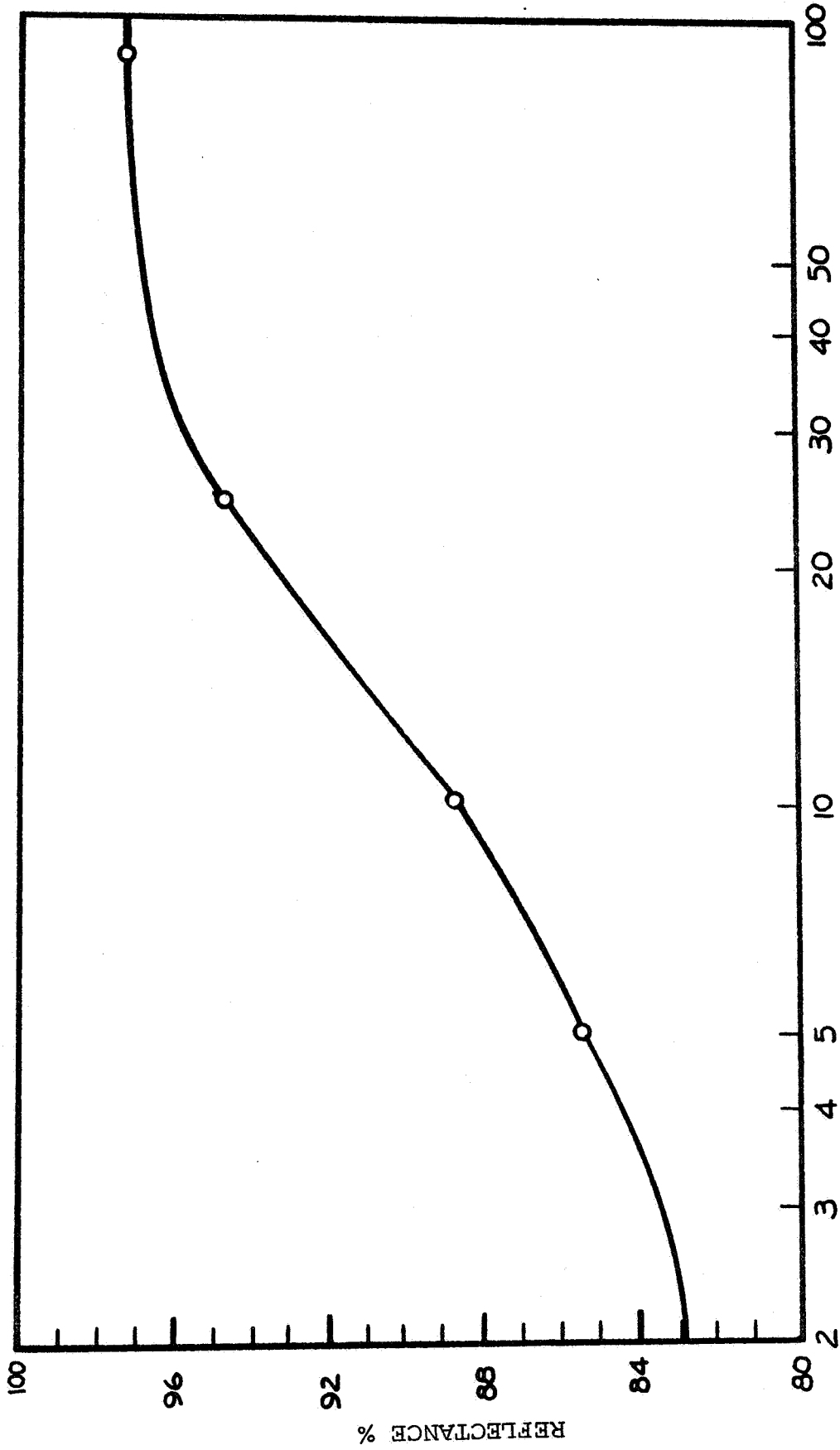


Fig. 5: EFFECT OF UV IRRADIATION IN THE IRIF ON BATCH A190 Zn<sub>2</sub>TiO<sub>4</sub>



TIME AFTER ADMISSION OF AIR (SECONDS)

Fig. 6: EFFECT OF ADMISSION OF AIR ON THE REFLECTANCE OF BATCH A-190  $Zn_2TiO_4$   
(at  $0.65 \mu$ )

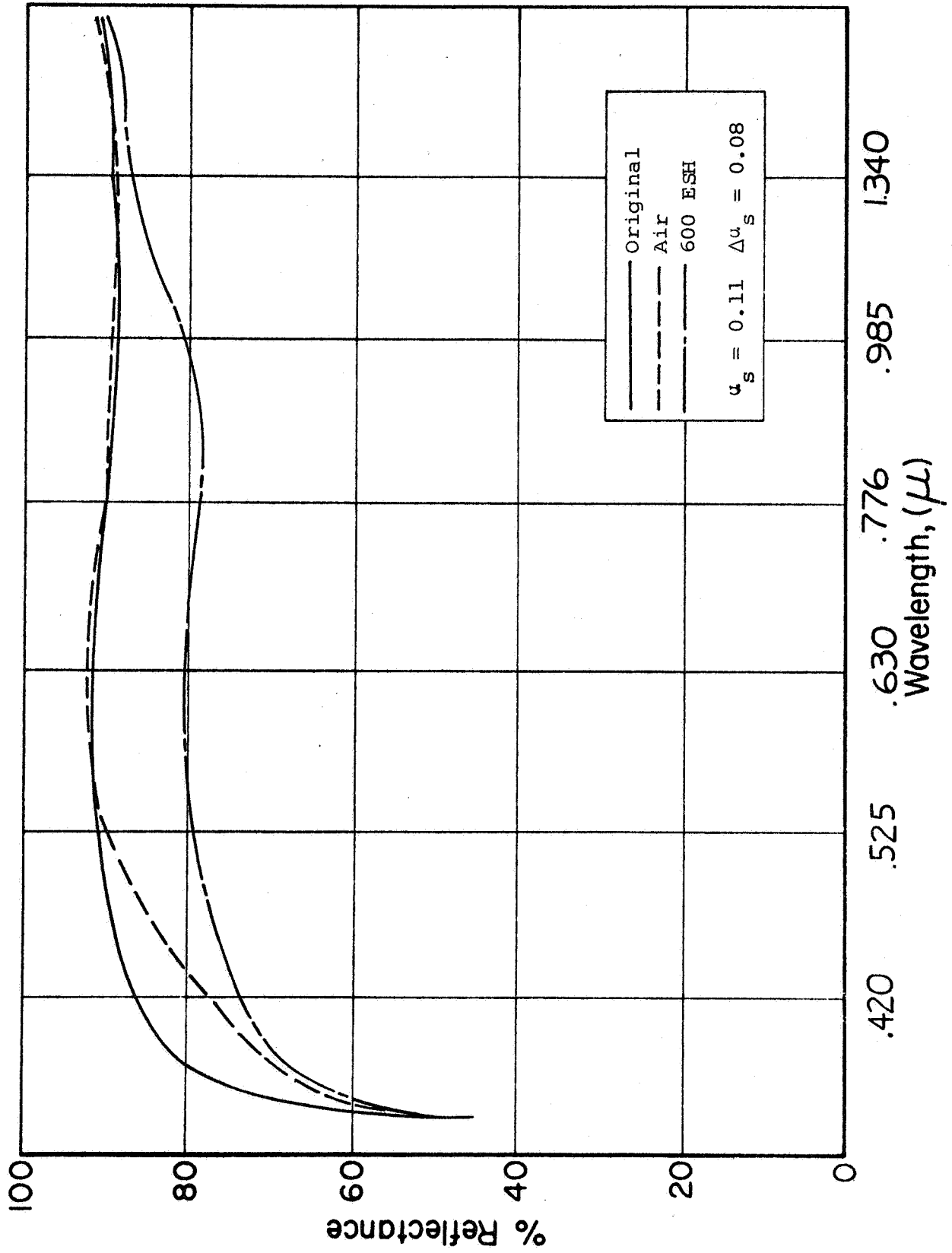


Fig. 7: EFFECT OF UV IRRADIATION IN THE IRIF ON NEW JERSEY ZINC'S A-54-2  $Zn_2TiO_4$

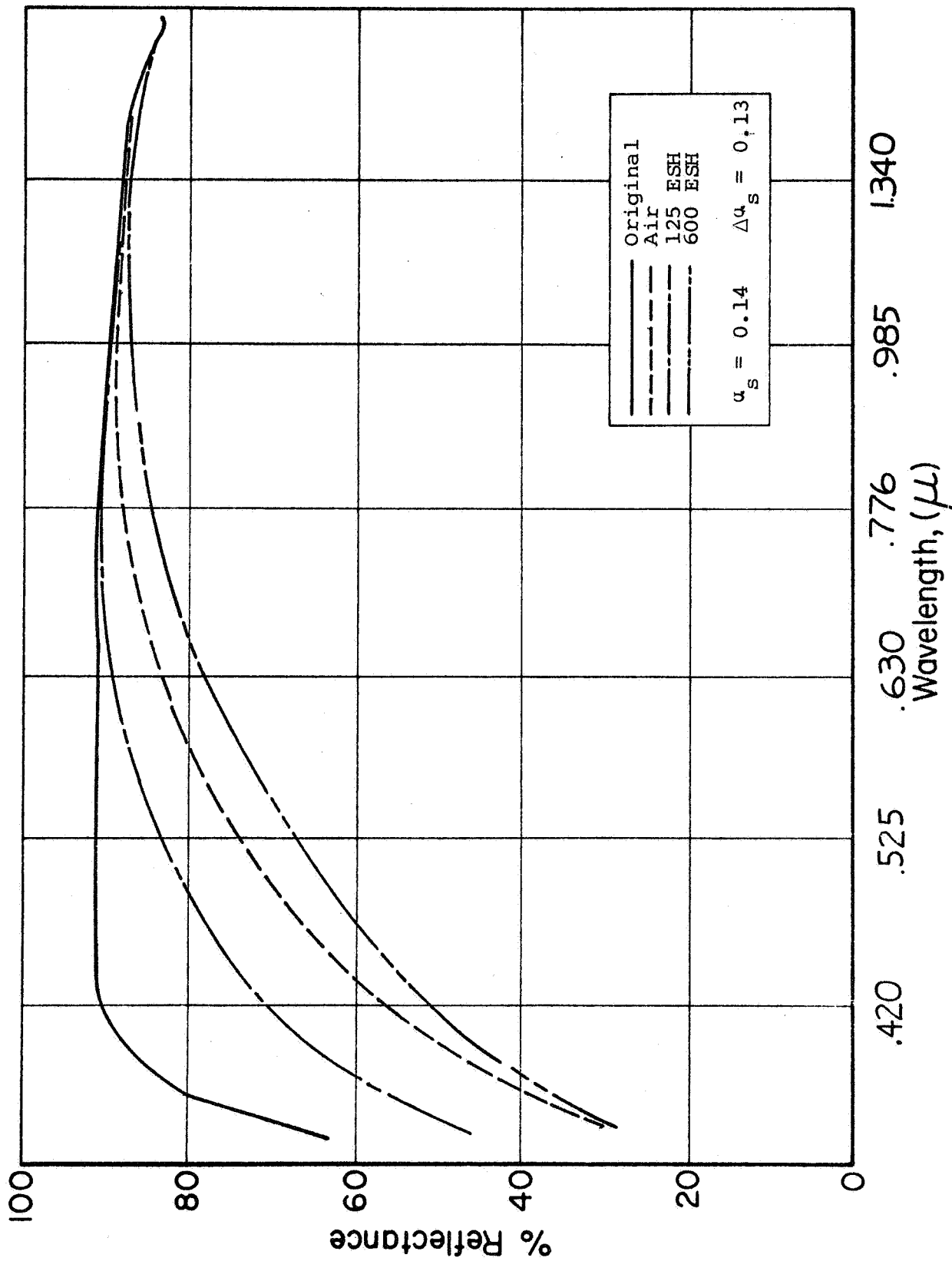


Fig. 8: EFFECT OF UV IRRADIATION IN THE IRIF ON TAM "CP" ZrO<sub>2</sub>

The damage to the experimental  $Zn_2TiO_4$  was manifested in a  $\Delta u_s$  of 0.093, 85% of which was almost instantly bleached on admission of air to the IRIF. The rate of bleaching at 6500 A on admission of air is shown in Figure 6. This bleaching curve is closely analogous to the rate curve presented for S-13 (an untreated ZnO-pigmented silicone paint) in a previous triannual Report (ref. 8).

Similar reflectance spectra for damaged  $Zn_2TiO_4$  were obtained with the commercial A-54-2 pigment. However, on admission of air to the IRIF, the commercial pigment exhibited greater permanent damage at 4000 A than the experimental pigment (see Figure 7).

The damage spectra of the "CP"  $ZrO_2$  is shown in Figure 8. The  $\Delta u_s$  of 0.132 was bleached by about 23% on admission of air. The  $\Delta u_s$  of 0.102 after admission of air is somewhat greater than is usually observed for an exposure of 600 ESH.

## 2. IRIF Test 7

The results of irradiation of seven  $Zn_2TiO_4$  specimens in test 7 are presented in Table 3. The corresponding reflectance spectra are shown in Figures 9 through 15. IRIF test 7 was for 1000 ESH of ultraviolet radiation and was performed at a nominal solar intensity of 6X.



Table 3

EFFECT OF 1000 ESH ULTRAVIOLET IRRADIATION IN VACUUM  
ON A SERIES OF ZINC ORTHOTITANATE POWDERS  
(IRIF Test 7; Solar Intensity 6X)

| Batch No. | Treatment                                    | Exposure, ESH | Solar Absorptance |            |            |                  |
|-----------|--|---------------|-------------------|------------|------------|------------------|
|           |  |               | $\alpha_1$        | $\alpha_2$ | $\alpha_s$ | $\Delta\alpha_s$ |
| A111      | 800°C for 16 hr                              | 0             | .087              | .033       | .120       | -                |
|           |  | 1000          | .112              | .058       | .170       | .050             |
| A190      | Batch A111 extracted with acetic acid        | 0             | .094              | .046       | .140       | -                |
|           |  | 1000          | .143              | .077       | .220       | .080             |
| A111-N    | Batch A111 extracted with NH <sub>4</sub> OH | 0             | .086              | .050       | .136       | -                |
|           |  | 1000          | .110              | .070       | .180       | .044             |
| A-190C    | Batch A190 calcined at 700°C for 16 hr       | 0             | .085              | .047       | .132       | -                |
|           |  | 1000          | .109              | .066       | .175       | .043             |
| A111-NC   | Batch A111-N calcined at 700°C for 16 hr     | 0             | .087              | .048       | .135       | -                |
|           |  | 1000          | .115              | .078       | .193       | .058             |
| A132      | 1050°C for 16 hr                             | 0             | .123              | .066       | .189       | -                |
|           |  | 1000          | .133              | .068       | .201       | .012             |
| A132-A    | Batch A132 extracted with acetic acid        | 0             | .126              | .079       | .205       | -                |
|           |  | 1000          | .126              | .079       | .205       | 0                |

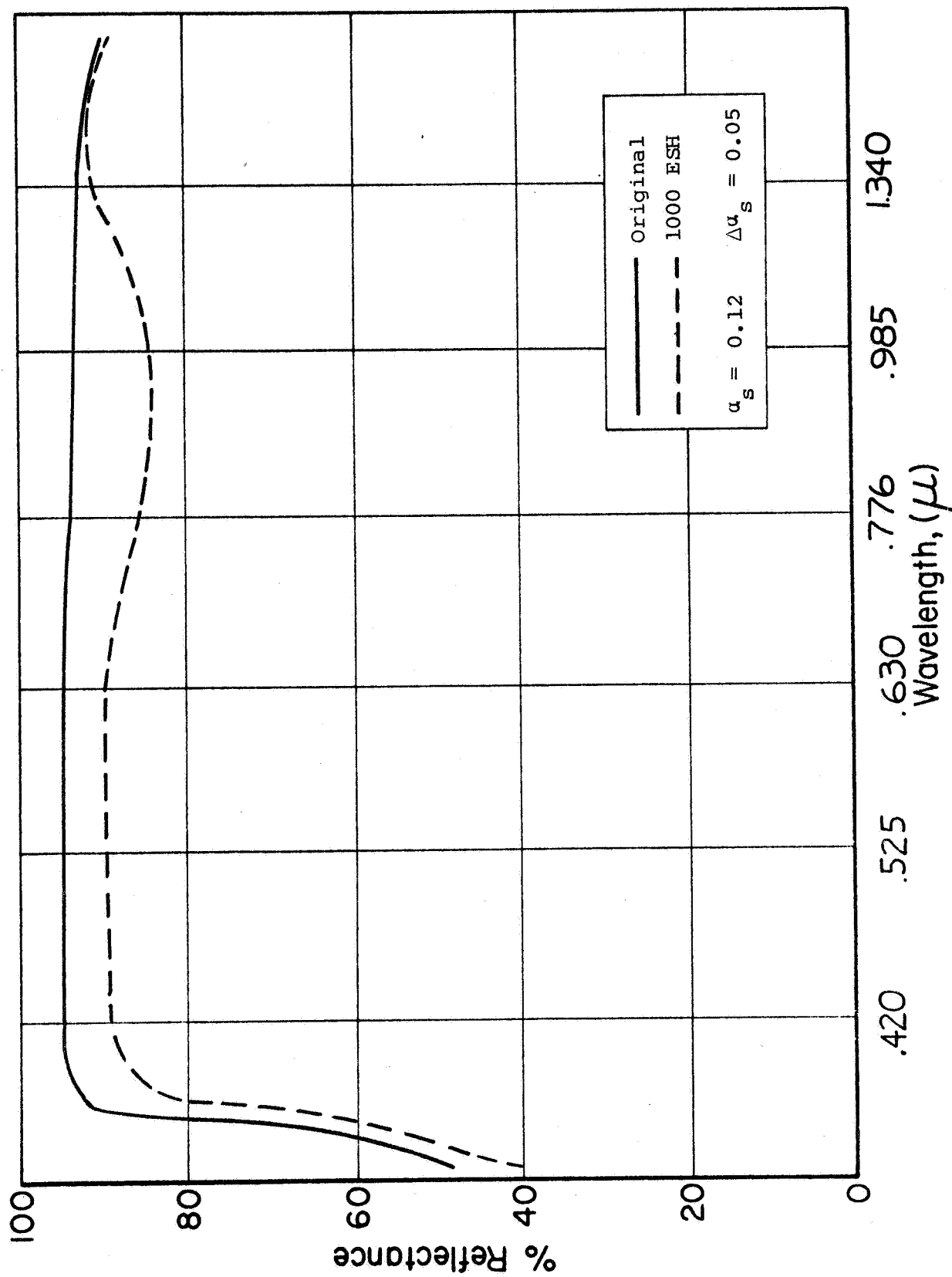


Fig. 9: EFFECT OF UV IRRADIATION IN THE IRIF ON BATCH ALL1 Zn<sub>2</sub>TiO<sub>4</sub> (800°C/16 hr)

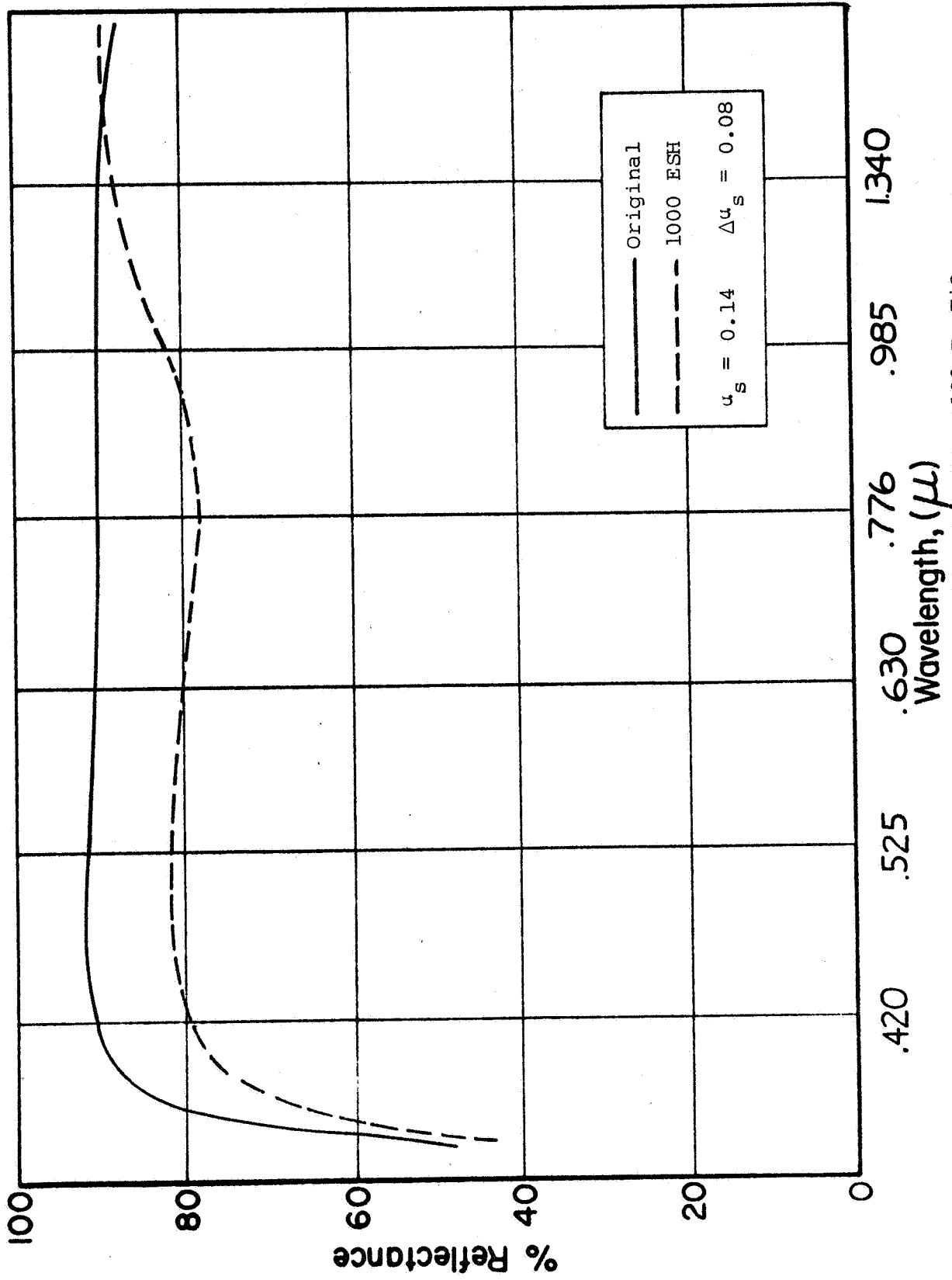


FIG. 10: EFFECT OF UV IRRADIATION IN THE IRIF ON BATCH A190  $Zn_2TiO_4$   
 (ALL EXTRACTED WITH ACETIC ACID)

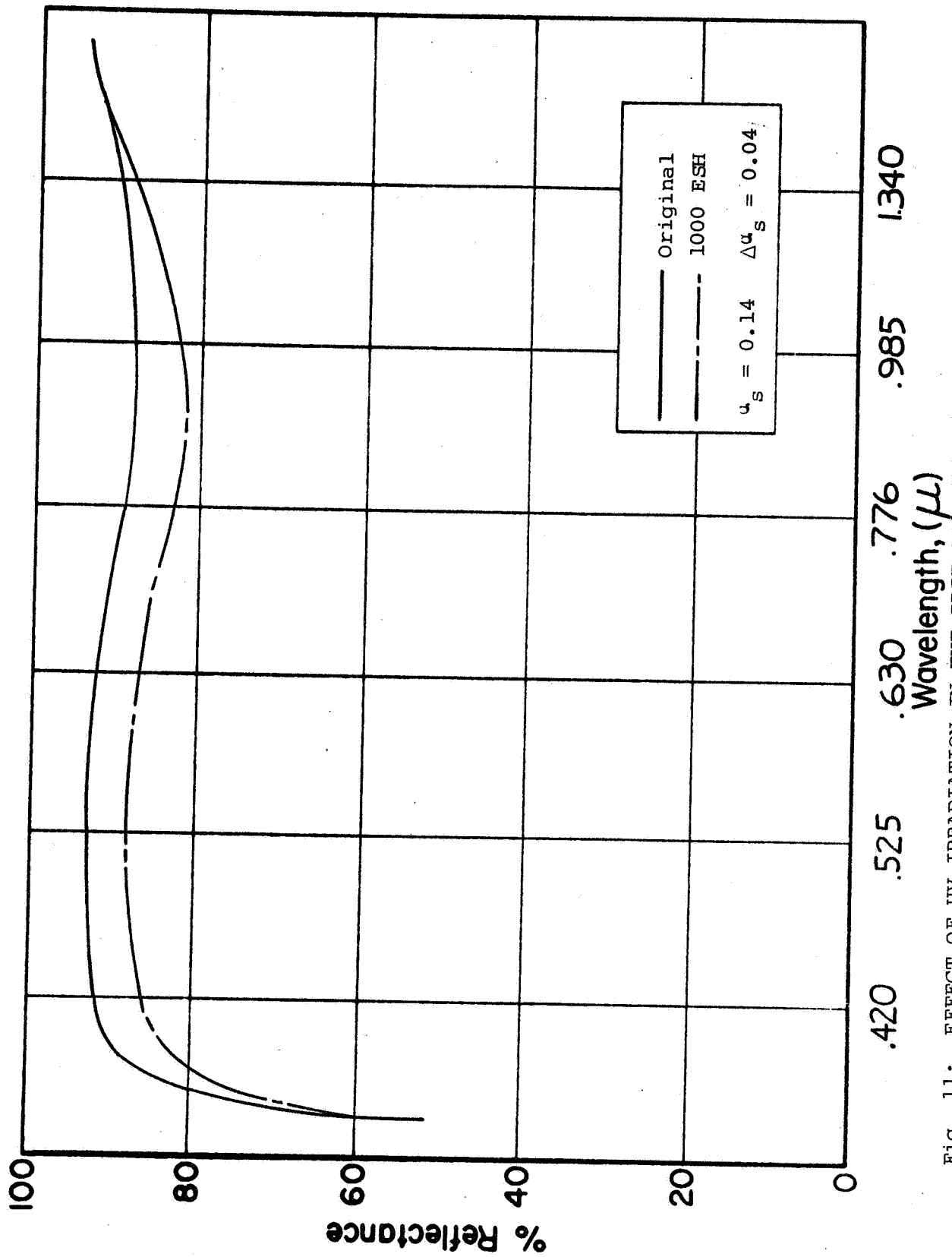


Fig. 11: EFFECT OF UV IRRADIATION IN THE IRIF ON BATCH ALL-N Zn<sub>2</sub>TiO<sub>4</sub>  
 (ALLI EXTRACTED WITH NH<sub>4</sub>OH)

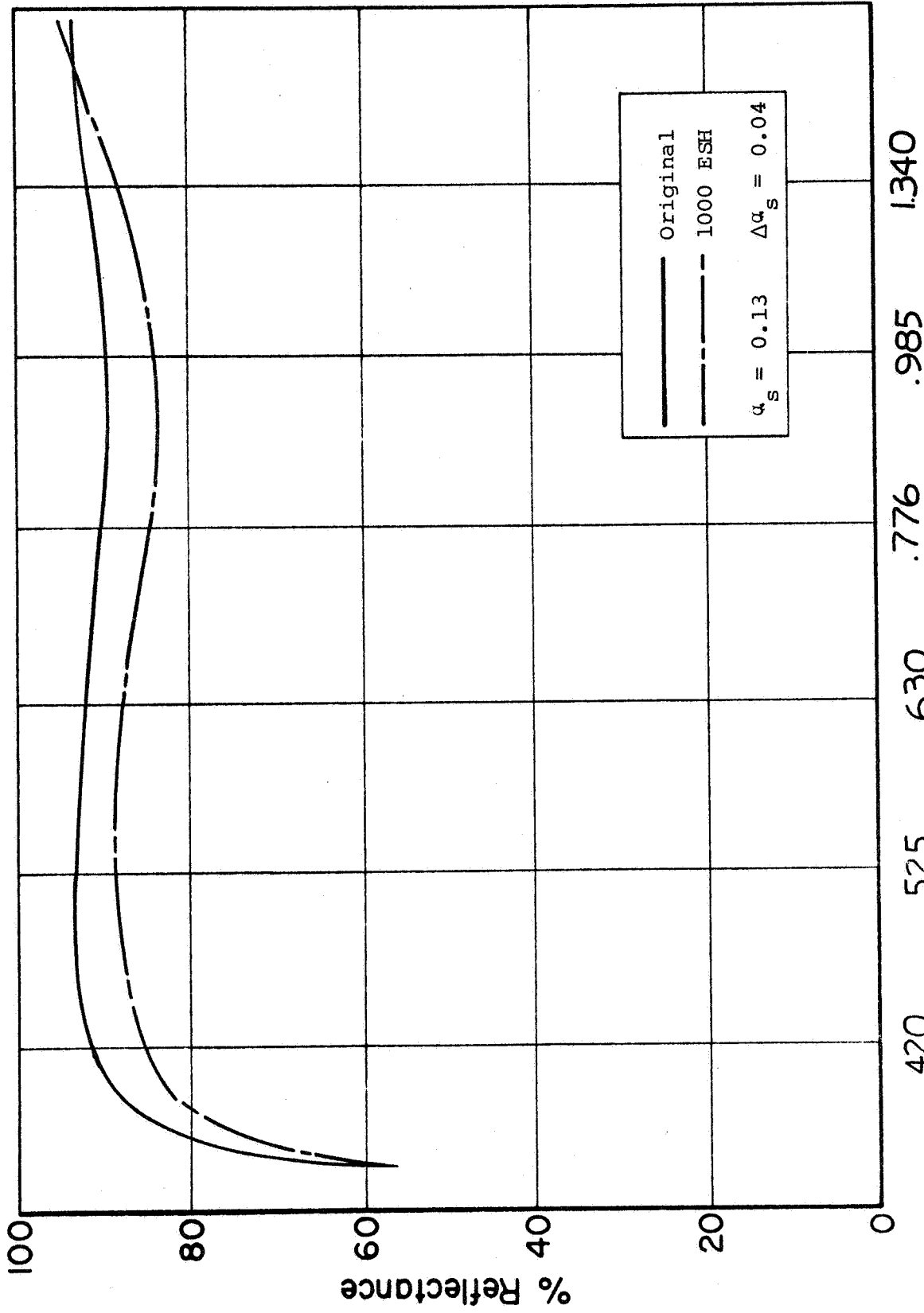


Fig. 12: EFFECT OF UV IRRADIATION IN THE IRIF ON BATCH A190-C Zn<sub>2</sub>TiO<sub>4</sub>  
 (A190 + 700°C/16 hr)

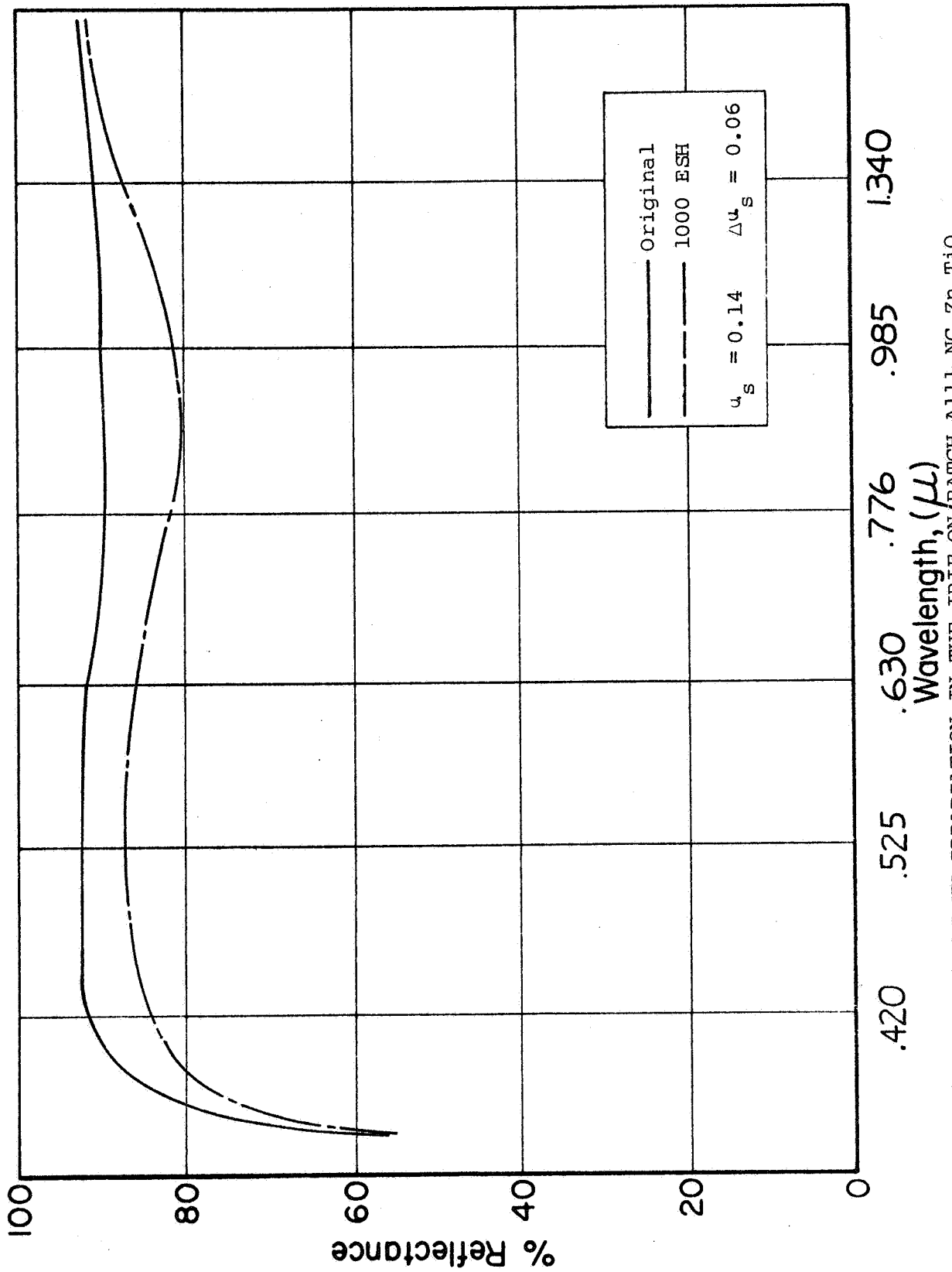


Fig. 13: EFFECT OF UV IRRADIATION IN THE IRIF ON BATCH ALL-N  $Zn_2TiO_4$   
 (All-N + 700°C/16 hr)

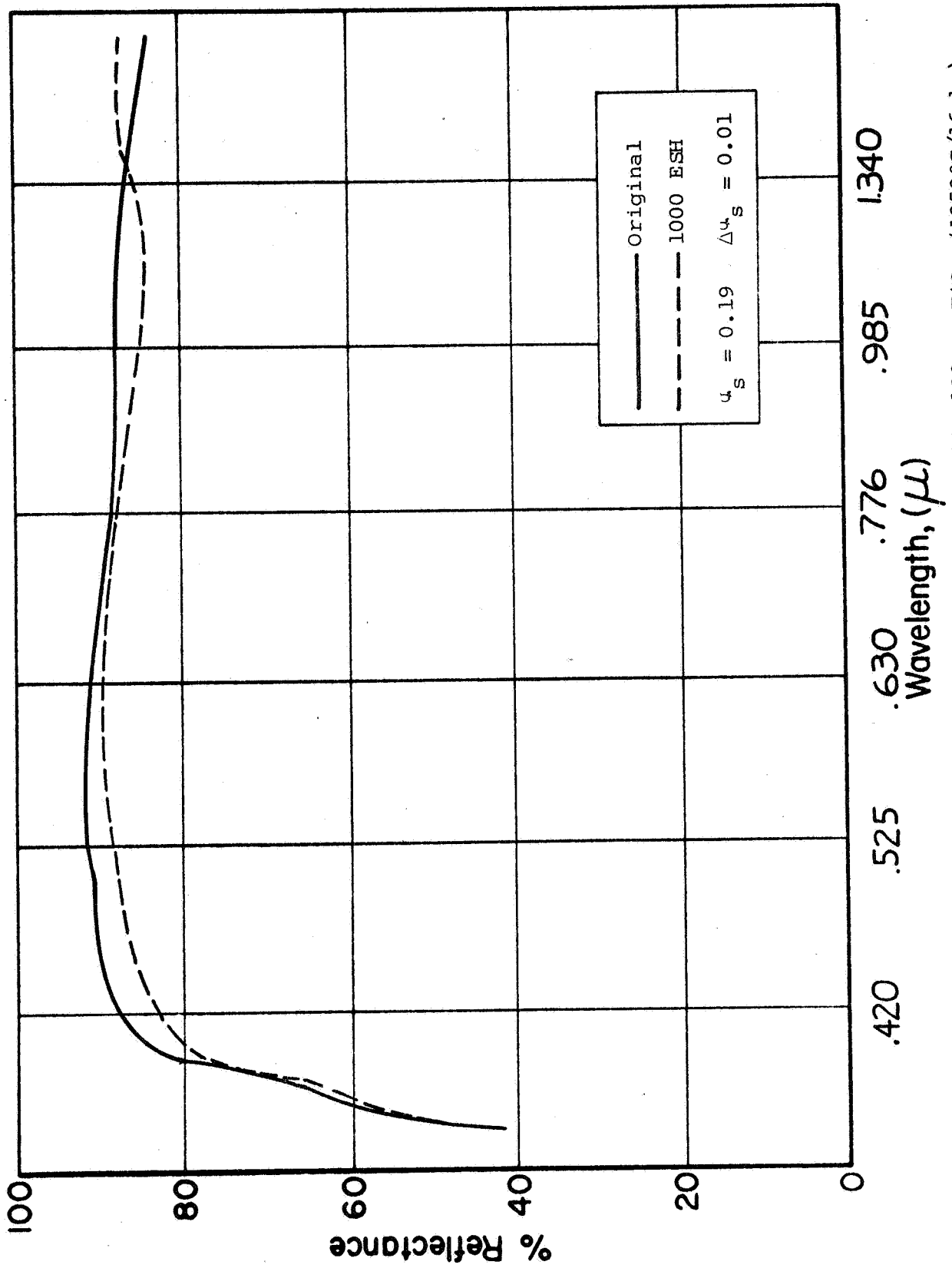


Fig. 14: EFFECT OF UV IRRADIATION IN THE IRIF ON BATCH Al32 Zn2TiO4 (1050°C/16 hr)

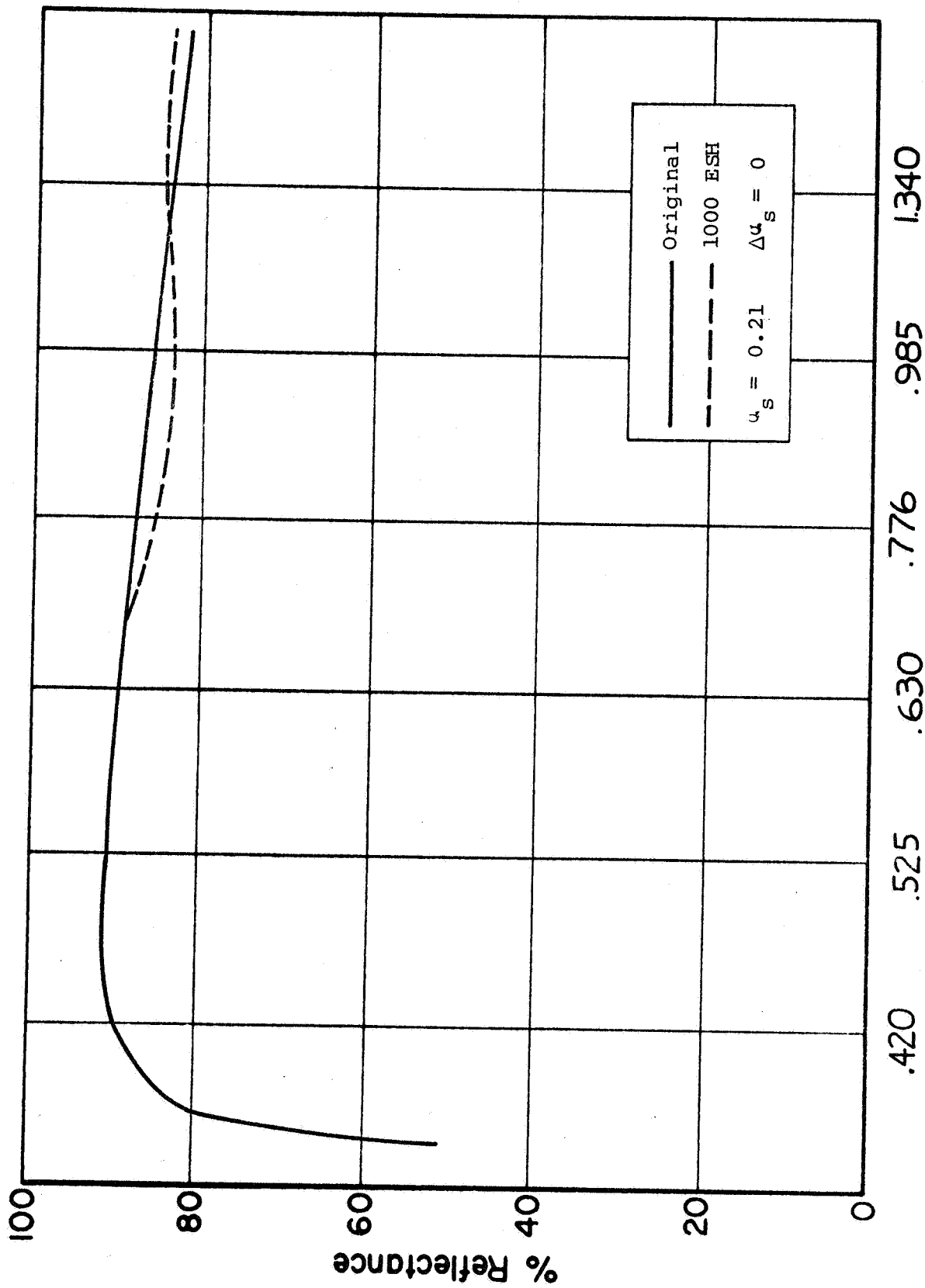


Fig. 15: EFFECT OF UV IRRADIATION IN THE IRIF ON BATCH A132-A  $Zn_2TiO_4$   
 (A132 EXTRACTED WITH ACETIC ACID)



Comparison of the data in Table 3 with those in Table 2 indicates that the 1000-ESH irradiation in test 7 may have been less severe than the 600-ESH irradiation in test 5. Although the A190 specimens were prepared at different times, the  $\Delta u_s$  that they exhibit in the two tests differ greatly: The  $\Delta u_s$ 's were 0.09 and 0.08 for tests 5 and 7, respectively (Figures 5 and 10).

Extraction of batch A111 with acetic acid caused an increase, whereas extraction with ammonium hydroxide caused a decrease in the resultant damage. On the other hand, recalcination of the two extracted specimens (Figures 12 and 13) had the opposite effect; the acid-extracted specimen showed an improvement on recalcination, whereas the alkali-extracted pigment exhibited increased damage when recalcined.

The randomness of these data suggest that the pigment preparation methods employed, such as variations in deagglomeration (grinding, milling, etc.) of the original and recalcined products, may have a profound effect on the stability of the resultant pigment. However, factors such as residual ZnO and unreacted titania, as well as incomplete neutralization of the acid and alkali used to extract the ZnO, may account for the effects noted.

The importance of complete reaction and/or high temperatures is emphasized by the results of irradiation of the  $Zn_2TiO_4$  prepared at 1050°C for 18 hours. The damage spectra of a virgin and an extracted specimen of the high-temperature  $Zn_2TiO_4$  are presented in Figures 14 and 15. Reaction at 1050°C produced a material

that exhibited a  $\Delta\alpha_s$  of only 0.01 in 1000 ESH of irradiation. The acetic acid-extracted specimen whose spectra is presented in Figure 15 exhibited a slight loss in reflectance in the 6400- to 12,000-A region only -- degradation that was countered by a reflectance increase, presumably due to a loss of adsorbed water, at wavelengths beyond 12,000 A, resulting in a  $\Delta\alpha_s$  of 0.

### 3. IRIF Test 12

Two  $Zn_2TiO_4$  specimens, three  $ZnTiO_3$  specimens, and a sulfate process-rutile-opacified borosilicate-glass enamel were irradiated for 600 and 1400 ESH in IRIF test 12 (Table 4).

The  $Zn_2TiO_4$  specimens were prepared from batch A132 by mulling the pigment in water. However, unlike the batch A132 specimens irradiated in IRIF test 7 (Figures 14 and 15), the specimens irradiated in test 12 exhibited severe degradation. Both the unextracted and extracted specimens exhibited  $\Delta\alpha_s$ 's of 0.06 in 1400 ESH (Figures 16 and 17). The discrepancy between the results of irradiation of the A132 specimens in tests 7 and 12 is believed to be due almost exclusively to the degree of grinding employed; the surface state defect concentration of the test 12 specimens is believed to be much greater than that of the test 7 specimens.

The data presented in Figures 18 through 20 for  $ZnTiO_3$  show that both extraction and recalcination have little effect on the stability of the original compound. The  $\Delta\alpha_s$  of 0.056 after 1400 ESH was increased to 0.062 and 0.065 on extraction and recalcination, respectively. These increases are more apt to be due to grinding differences than to the effects of the treatment employed.

Table 4

EFFECT OF ULTRAVIOLET IRRADIATION IN VACUUM  
ON SEVERAL ZINC TITANATES  
(IRIF Test 12; Solar Intensity 6X)

| Sample | Zinc Titanate   | Treatment                                    | Exposure,<br>ESH | Solar Absorptance |            |                  |
|--------|---|--|------------------|-------------------|------------|------------------|
|        |   |  |                  | $\alpha_1$        | $\alpha_2$ | $\Delta\alpha_s$ |
| 5      | Ortho<br>Al32   | Reacted at 1050°C<br>for 16 hr               | 0                | .114              | .061       | .175             |
|        |   |  | 600              | .140              | .082       | .222             |
|        |   |  | 1400             | .147              | .089       | .236             |
| 1      | Ortho<br>Al32-A   | Pigment 5 extracted<br>with acetic acid      | 0                | .113              | .073       | .186             |
|        |   |  | 600              | .139              | .091       | .230             |
|        |   |  | 1400             | .147              | .095       | .242             |
| 11     | Meta<br>Al29  | Not extracted; Reacted<br>at 850°C for 17 hr | 0                | .121              | .055       | .186             |
|        |   |  | 600              | .145              | .078       | .223             |
|        |   |  | 1400             | .154              | .088       | .242             |
| 10     | Meta<br>Al29-A  | Extracted with<br>acetic acid                | 0                | .125              | .041       | .166             |
|        |   |  | 600              | .145              | .072       | .217             |
|        |   |  | 1400             | .148              | .080       | .228             |
| 4      | Meta<br>Al29-AC   | Pigment 10 calcined<br>16 hr at 800°C        | 0                | .122              | .052       | .174             |
|        |   |  | 600              | .149              | .087       | .236             |
|        |   |  | 1400             | .150              | .089       | .239             |
| 2      | Porcelain<br>(Rutile opacified<br>borosilicate glass;<br>PVC = 14%) |  | 0                | .163              | .143       | .306             |
|        |   |  | 600              | .164              | .141       | .305             |
|        |   |  | 1400             | .168              | .144       | .313             |

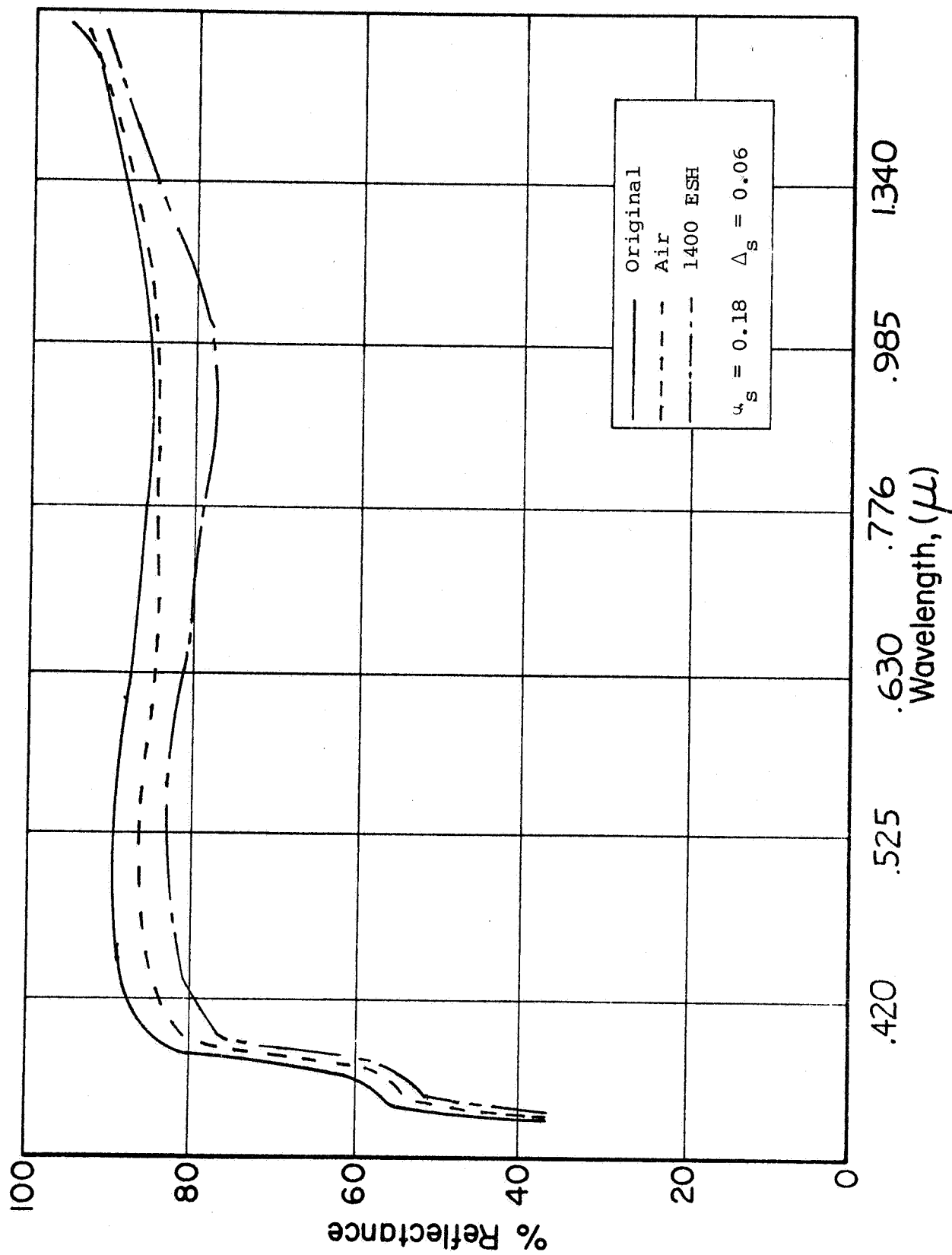


Fig. 16: EFFECT OF UV IRRADIATION IN THE IRIF ON BATCH Al32 Zn<sub>2</sub>TiO<sub>4</sub> (1050°C/16 hr)

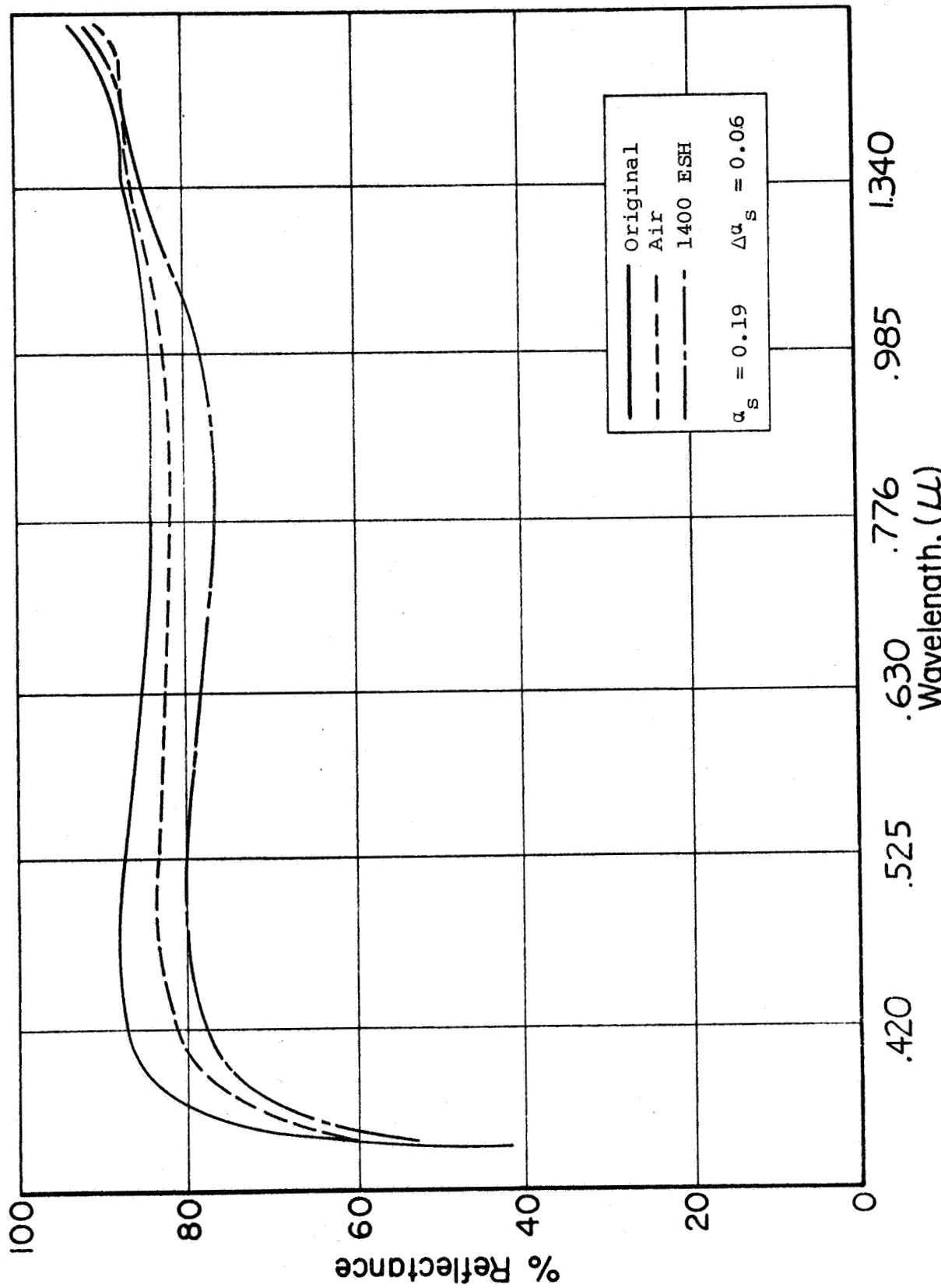


Fig. 17: EFFECT OF UV IRRADIATION IN THE IRIF ON BATCH A132-A  $Zn_2TiO_4$   
(A132 EXTRACTED WITH ACETIC ACID)

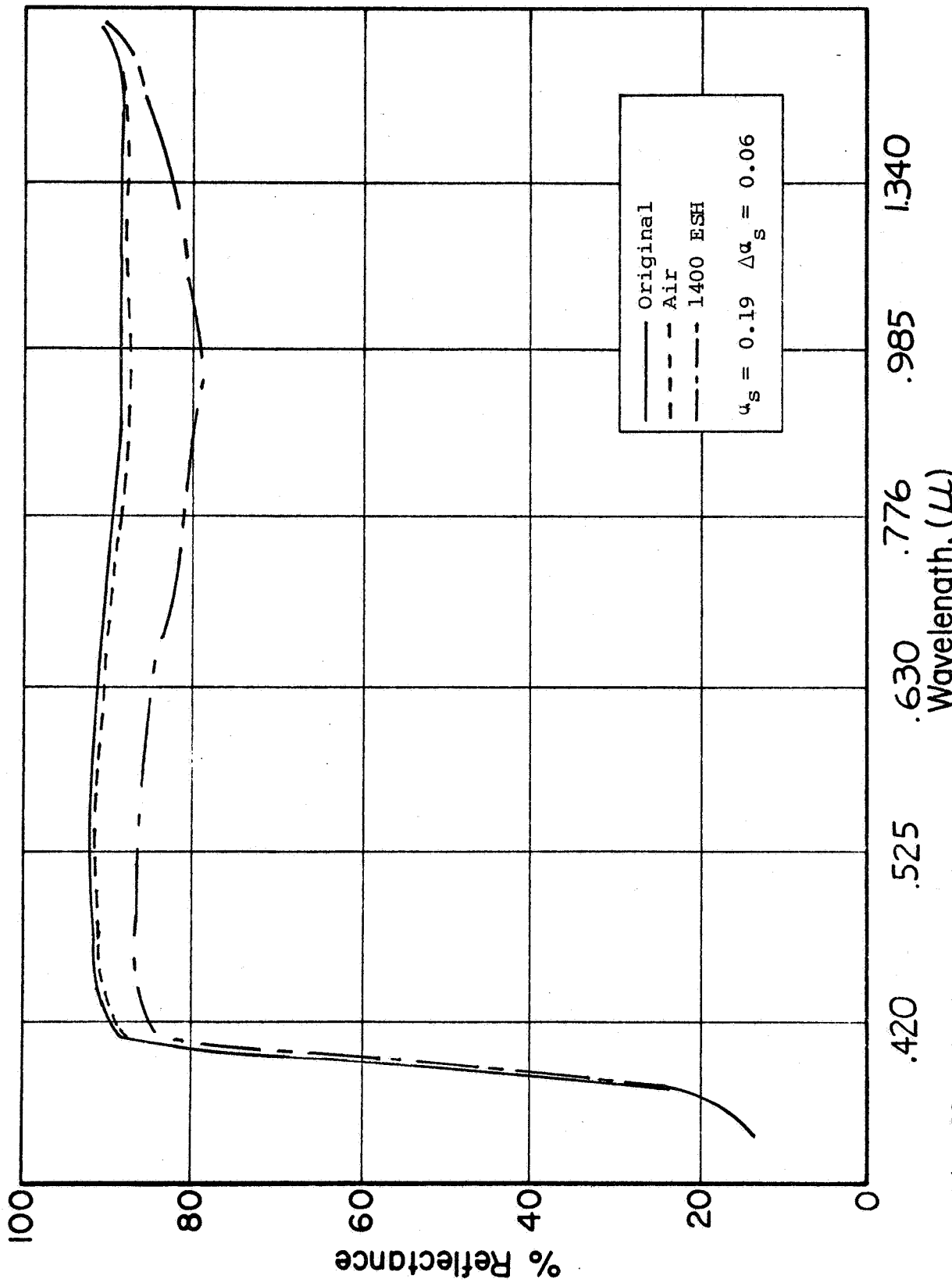


Fig. 18: EFFECT OF UV IRRADIATION IN THE IR.F OF BATCH A129 ZnTiO<sub>3</sub> (850°C/15 hr)

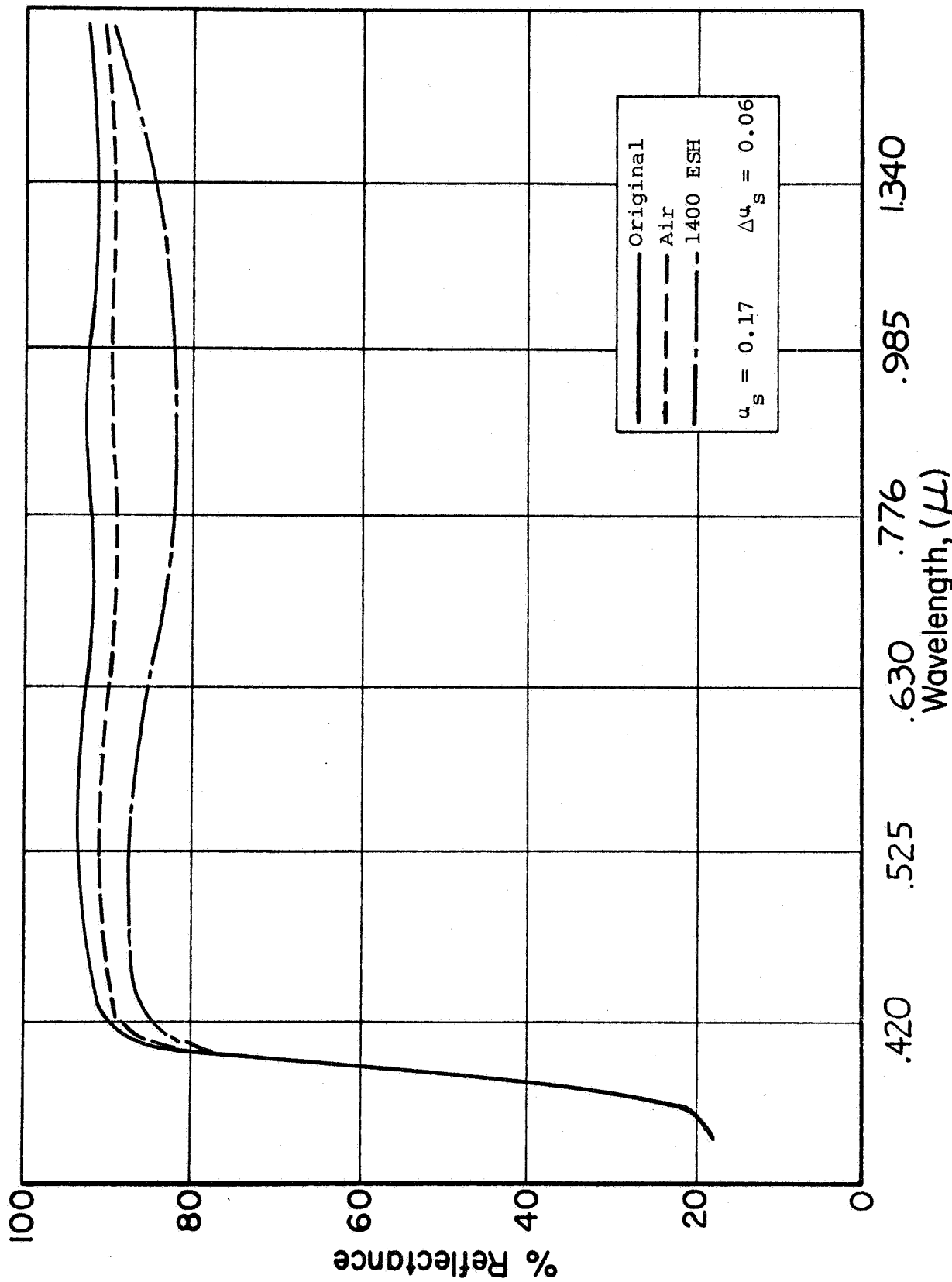


Fig. 19: EFFECT OF UV IRRADIATION IN THE IRIF ON BATCH A129-A ZnTiO<sub>3</sub>  
 (A129 EXTRACTED WITH ACETIC ACID)

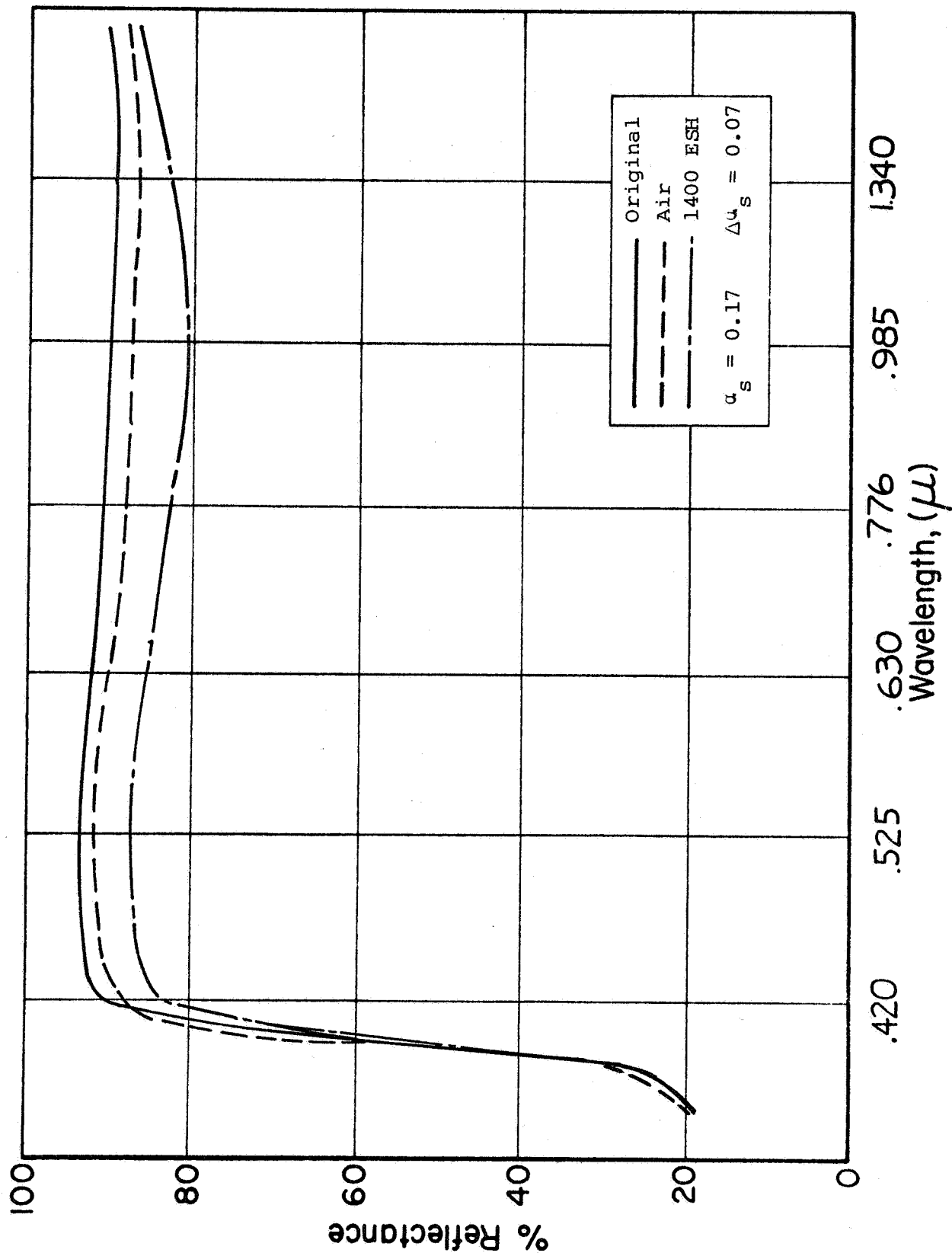


Fig. 20: EFFECT OF UV IRRADIATION IN THE IRIF ON BATCH A129-AC (A129-A + 800°C/16 hr)



The excellent stability of the porcelain specimen, a rutile-opacified borosilicate glass enamel, is consistent with previous data on porcelains. The  $\Delta\alpha_s$  of 0.007 after 1400 ESH is shown graphically in Figure 21. Since this specimen is a commercial frit that was selected at random, without regard to either optimization of the ingredients for stability or the opacifier for solar reflectance, we believe that porcelains hold much promise for application where stable systems are required for use at elevated temperatures.

We currently plan to utilize porcelains as control specimens in selected tests to ascertain the presence, or absence, of contamination during the IRIF space-simulation tests.

### III. THE SOLID-STATE CHEMISTRY OF ZINC TITANATES

#### A. Background Discussion

##### 1. The Pigment in a Space Coating

The pigment particle in a space coating is a small crystal; thus it would appear that all the techniques of solid-state physics could be applied to it. Many techniques can be used, but those of special interest to us are X-ray spectra, optical (reflection, absorption, or emission), magnetic resonance, magnetic susceptibility, and electrical properties, including photoconductivity and changes in dielectric properties.

In addition to the starting material, it is important to study and understand the reactions induced by the solar radiation environment. Radiation damage is a primary field of investigation in solid-state chemistry and also has been a

IIT RESEARCH INSTITUTE

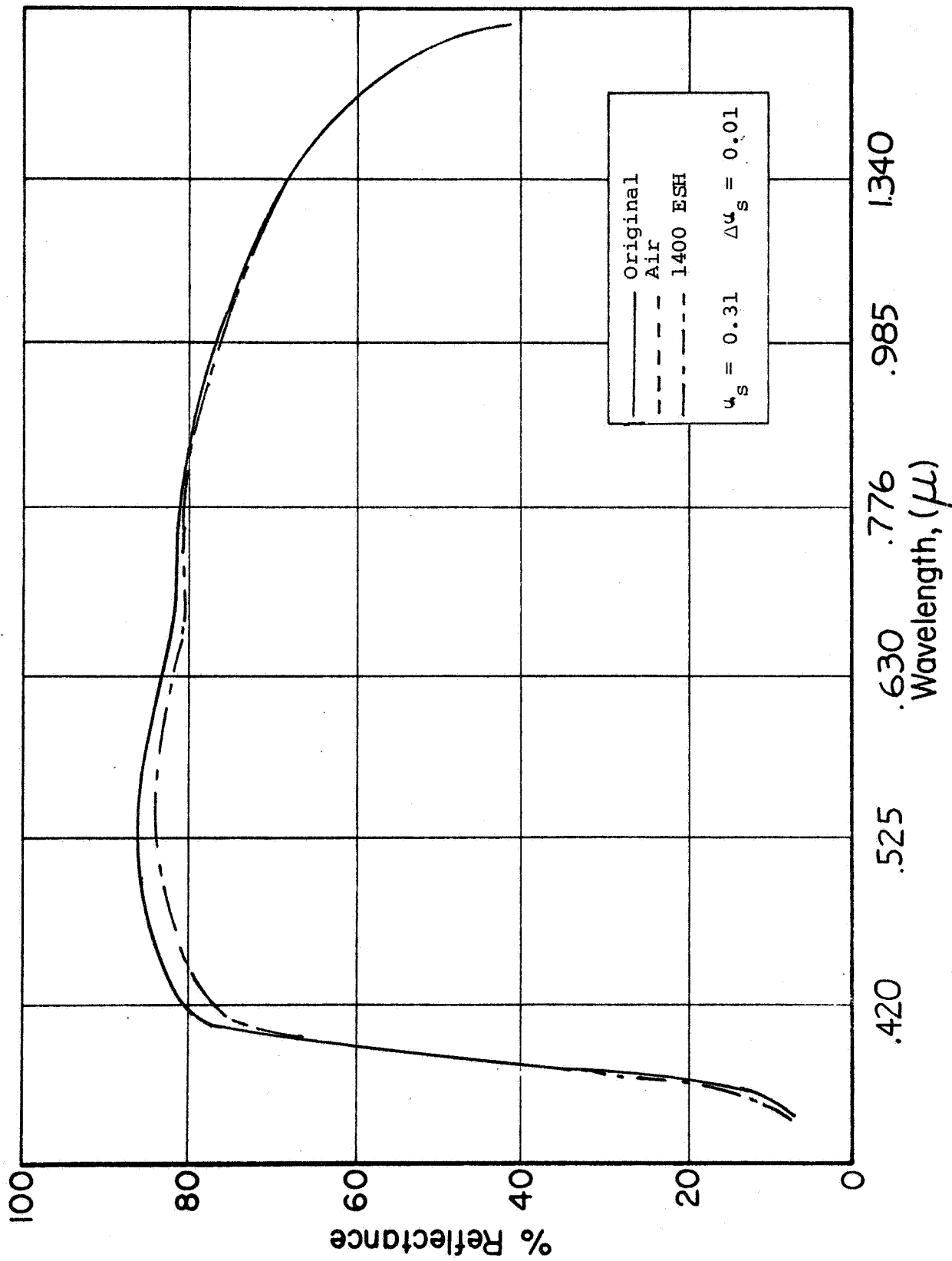


Fig. 21: EFFECT OF UV IRRADIATION IN THE IRIF ON A RUTILE OPAFICIFIED PORCELAIN ENAMEL

diagnostic method for studying crystalline defects. Radiation effects can involve only a very small portion of the numerous ions in a solid! This fraction can range from 1 ppm to 1 part per thousand, which is at the limit of the ordinary range of chemical purity. It is advantageous to have a detection method that is sensitive only to the defects and not to the intrinsic properties, so precise measurements to obtain a small change in a large quantity are not required. An example is the effect of a magnetic impurity ion in a crystal lattice. The lattice parameter as determined by X-ray studies is changed only slightly when defects are present; magnetic susceptibility changes slightly, but the paramagnetic resonance is a property only of the defects.

## 2. Anisotropy

The theory for an observation of a physical property depends on a quantum mechanical operator. This operator retains the property of a vector corresponding to the classical quantity of interest. Suitable averages over the volume of the sample and time are required to obtain a value corresponding to the quantity as measured. Crystalline solids are characterized by certain unit directions along which unit cells are repeated to fill all space. The unique directions may be equivalent or nonequivalent. Many symmetry operations for a cubic crystal transform the crystal into itself. However, a material such as calcite is characterized by fewer symmetry operations since one axis is different than the other two. A crystal, as observed by most ordinary optical methods,

may be isotropic or anisotropic. However, even though the crystal is isotropic, individual sites may not be isotropic or the local symmetry may be destroyed by applied fields such as stress or electric or magnetic fields; for example, the electrical conductivity is the same for all directions in a magnesium oxide (MgO) crystal, but one principal direction is different from the other two in ZnO. The anisotropy due to low site symmetry is particularly important in electron paramagnetic resonance experiments.

If a single crystal cannot be obtained, the polycrystalline powder must be studied. There must be a sufficient number of particles to provide a completely random distribution. Such experiments are difficult to interpret because a model must be assumed and then a spectrum calculated as a function of crystal orientation. The observed spectrum is the average over all orientations weighted by the probability of their occurrence. A number of assumptions may be consistent with a single observed spectrum. However, partially oriented samples can sometimes be prepared to eliminate some possible models.

For a rapidly tumbling molecule in solution, the anisotropic effects average to zero, but for rigid solids, anisotropic effects produce a line broadening. This is one example of inhomogeneous broadening, as contrasted with other types of broadening, termed homogeneous. Most interactions can be divided into isotropic and anisotropic parts. A resonance type of phenomenon is usually quite a sensitive method, but broadening effects reduce sensitivity.

Inhomogeneous broadening due to anisotropy is removed by using single crystals. The preparation of a single crystal is almost always desirable, but many problems involving thermal properties, chemical purity, and crystalline perfection may be encountered.

### 3. Impurities and Crystalline Perfection

Much has been written about purity in solid-state studies. Intrinsic crystal imperfections composed of lattice vacancies and interstitials can play a role similar to that of impurities. In chemical language, impurities may change valence or form complex ions, which are often called centers and participate in the trapping of holes or electrons. Complex reactions involving photochemical and thermal effects may occur. Electrical charge in a "small region" of the crystal must always balance. Relations analogous to chemical equilibria and size considerations must be considered. Structural and purity effects are not separable.

The point here is that a low concentration of impurity can have a very large effect. Semiquantitative chemical analysis detects concentrations below 1%. Higher accuracy can be obtained if samples are large, but those of interest are usually small. Natural structural defects in ordinary samples can range in parts per million or less and are usually difficult to detect except by a decoration method. The important range in many materials is from 1 part per thousand to 1 ppm. At higher concentrations, the basic structure begins to break down and interactions between centers complicate interpretation. At lower concentrations, the effects of interest blend into other less

controllable factors and detection can be difficult. A one-electron-type optical transition in a defect at a concentration of  $10^{-3}$  mole can make a crystal opaque. Concentrations much below this can reduce the reflection of a powder.

#### 4. Surface States

The surface of a crystal does not represent the interior. The energy of atoms at the surface is higher than that in the interior, particularly in polyvalent ionic crystals. An anisotropic effect is introduced because different crystal faces have different relative numbers of ions with unique spacings. This has been verified in many ways -- two examples are electron emission and catalytic effects.

Surface species participate in chemical reactions that would not normally occur in the bulk solid, and in fact, the reactions of solid materials involve surface considerations. Physical adsorption on the surface is known to be reasonably reversible, and there are more tightly bound states called chemical absorption. In fact, there are bonds between atoms in absorbed species that do not occur in the bulk solid. An example is oxygen absorbed on ZnO. It appears that the stable molecule is  $O_2^-$  (ref. 19), as indicated by magnetic resonance. Similarly,  $O_2^-$  is produced on MgO if it is irradiated with ultraviolet. The species  $O_2^-$  is known in solids such as alkali halides. In this case,  $O_2$  is soluble at few atmospheres with sufficient time and temperature. Irradiation with gamma rays produces the ion  $O_2^-$ .

However, MgO is most exceptional because carbon monoxide (normally diamagnetic) forms a paramagnetic radical (uncharged) on the surface. This would not be anticipated from MgO and CO reactions but is consistent with knowledge of catalytic processes. The separation between bulk solid surface and surface species is of course somewhat arbitrary.

In space coatings the situation is complicated because the surface is between two solids and the molecules of the vehicle are more complex. Nevertheless, it is not surprising to find unexpected reactions at the surface that are dependent on an interface between two solid layers.

#### 5. Radiation Effects and Decoration of Defects

Frequently lattice imperfections, impurities, and surface states show no easily measurable properties. Ionization processes can separate electrons and holes that may be stabilized at new locations if energies and kinetics are favorable. Frequently this leads to systems with a magnetic moment so that paramagnetic resonance is appreciable. Some of these states may be metastable. High-energy radiations such as gamma-rays or X-rays are very effective. Ultraviolet can be effective if even the smallest optical adsorption is present in the host lattice. More dramatic results are obtained by long irradiation at high energies, which generate defects rather than decorate existing ones. Often this reveals impurities and allows accurate studies at high concentration, but the

application of these ideas to the relatively low energy of photodegradation must be considered with care.

#### 6. Interaction of Surface and Bulk Properties

The total effect of the solid and vehicle is not entirely the sum of the bulk and surface effects. The surface states behave as impurities or defects and may trap electrons and holes. They may influence the occupation of the valence and conduction bands. The photoconduction of single crystals of ZnO depends on the absorbed gasses, particularly oxygen (ref. 20). The net effect is a surface layer of excess electrons. The occupation of the conduction band in the bulk is affected by the surface states. Such interactions are well known in semiconductors (silicon and germanium). Indeed this provides a mechanism for altering bulk properties in a complicated manner. Impurities in the bulk may also become "activated" when suitable surface states are occupied.

#### B. Proposed Experiments

The research program for these zinc titanates is divided into three main categories, designated as phases:

- I. Materials preparation
- II. Properties of observable species
- III. Investigation of systems.

No one phase is independent of the other, and the sophistication of each must develop concurrently. Complete coordination is required to obtain consistent results.



## 1. Materials Preparation

Pure polycrystalline powders of  $\text{ZnTiO}_3$  and  $\text{Zn}_2\text{TiO}_4$  must be prepared. The important objective is that they contain a single phase (and a single crystalline habit) and have a known composition. Semiquantitative chemical analysis would indicate impurities with a concentration above 1 ppm. Since there are on the order of a hundred elements in a variety of valence states, a judicious choice of analysis for the most probable impurities must be made. Known purity is as important as achieving the ultimate purity. However, several impurities may complement each other to make the total damage more or less than that of the individual impurities. A highly impure material is probably not a reproducible material.

An investigation of possible methods of crystal growth will be made. If any of these seem to indicate a convenient preparation, single-crystal growth will be attempted. Most probably this will involve a high-temperature method. Chemical purity will not be sacrificed because of its important influence on crystal growth.

## 2. Properties of Observable Species

This is essentially a qualitative analysis to detect bulk or host crystal imperfections as grown and as detected by decoration methods. The methods are:

### a. Optical

- . Optical reflection of powders
- . Specular reflection of single crystals
- . Optical transmission of pressed pellets or liquid suspensions.

b. Luminescent

- . Phosphorescence of impure and pure materials will be sought.
- . Low temperatures will be employed to increase the yield, but quantitative yields will be measured only as part of phase III. It is anticipated that pure materials will have the least luminescence.
- . Thermoluminescence will be qualitatively sought.

c. Magnetic

Electron magnetic resonance of powders and single crystals will be sought. Resonance should not be present in pure materials. Irradiation will be used to decorate defects and to find the most important hole and electron traps in the bulk. Experiments will be performed on powders with specially treated surfaces; O<sub>2</sub>, N<sub>2</sub>, CO, and C<sub>2</sub>H<sub>4</sub>. The minimum energy for development of a defect will be estimated.

d. Dielectric

In order to determine the role of the conduction band and transitions to the conduction band, photoconductivity will be considered. This requires two separate approaches, depending on the material state. If single crystals are available, the range of conductivity will be determined from the literature or crude experiments. Photoconductivity will be measured if the properties match the proper ranges of available equipment. For powders, methods based on measurements of high-frequency dielectric constants will be investigated. These investigations will be directed to developing techniques suitable for studying surface

IIT RESEARCH INSTITUTE

states and to eliminating problems associated with polarization, anisotropy, and contacts. It is anticipated that high sensitivity can be achieved if the time constants of the states are suitable.

### 3. Investigation of Systems

This is a quantitative program and, to a large extent, presupposes the success of the two preceding phases. However, it is primarily directed to the study of useful coatings. Calibration problems are significant.

Energy deposition will be measured as a function of wavelength, and primarily ultraviolet will be utilized. This will be correlated with the areas of absorption bands generated in the coatings. The kinetics of reaction will be investigated. Those centers that are important but are more easily studied by techniques other than optical reflection will be observed by employing methods used in phase II.

### IV. PHYSICAL SENSITIVITY OF SILICATE-TREATED ZINC OXIDE

The sensitivity of pure ZnO to mechanical distortion has been discussed in numerous communications on this and other programs dealing with the development of space-stable coatings. We examined the problem of mechanical distortion of zinc oxide in a program for the Jet Propulsion Laboratory (Contract 950746) in late 1965 (ref. 21). No detectable electron spin resonance signal was observed on SP500 ZnO samples that were mechanically yellowed. Damaged specimens were observed to possess a rather narrow, intense absorption band centered at about 3750 Å.

IIT RESEARCH INSTITUTE

In the studies cited as well as in both previous and later work, we have observed that mechanically yellowed specimens exhibit greater degradation when irradiated with ultraviolet in vacuum than samples that are not mechanically damaged. This is not surprising since the increased absorption also increases the probability of the occurrence of photolytic effects. Although the mechanism is not well understood at this time, Gilligan (ref. 21) has attributed it to the creation of interstitial zinc.

Our previous experience with the physical sensitivity of ZnO led us to examine the effect of grinding, and the physical distortion so produced, on the silicate-treated SP500 ZnO employed in IITRI's thermal-control coating designated S-13G. A series of S-13G paints was prepared from the same batch of silicate-treated SP500 ZnO; the only difference was the manner in which the dried, treated powder was conditioned for grinding (manufacturing) into the paint. The data obtained are presented in Table 5 and Figures 22 through 26.

Examination of these data show that the stability to ultraviolet irradiation in vacuum is an inverse function of the shear applied to the dry, silicate-treated pigment prior to wet-grinding. (Excessive wet-grinding is also known to decrease stability.) A fivefold increase in damage, as measured by  $\Delta u_s$ , was observed between the paint prepared from pigment that was only sifted (#6, Figure 22) and the specimen that was prepared from pigment that was hand-mulled prior to wet-grinding (#7, Figure 25).

Table 5  
EFFECT OF ULTRAVIOLET IRRADIATION  
IN VACUUM ON S-13G PAINTS\*  
(IRIF Test 12)

| Specimen | Treatment  | Exposure,<br>ESH | Solar Absorptance |       |       |              |
|----------|--|------------------|-------------------|-------|-------|--------------|
|          |  |                  | $u_1$             | $u_2$ | $u_s$ | $\Delta u_s$ |
| 6        | Pigment sifted only;<br>paint ground 3 hr          | 0                | .148              | .092  | .240  | -            |
|          |  | 600              | .155              | .087  | .245  | .005         |
|          |  | 1400             | .161              | .090  | .251  | .011         |
| 12       | Pigment not sifted;<br>paint ground 7 hr           | 0                | .128              | .087  | .215  | -            |
|          |  | 600              | .139              | .085  | .224  | .009         |
|          |  | 1400             | .151              | .085  | .236  | .021         |
| 8        | Pigment dry-ground<br>30 min; Paint ground<br>3 hr | 0                | .134              | .087  | .221  | -            |
|          |  | 600              | .153              | .092  | .245  | .024         |
|          |  | 1400             | .159              | .092  | .251  | .030         |
| 7        | Pigment hand-mulled;<br>paint ground 3 hr          | 0                | .147              | .111  | .258  | -            |
|          |  | 600              | .169              | .109  | .278  | .020         |
|          |  | 1400             | .189              | .116  | .305  | .047         |
| 9        | Ends from #7 remulled;<br>paint ground 5 hr        | 0                | .140              | .093  | .233  | -            |
|          |  | 600              | .167              | .099  | .266  | .033         |
|          |  | 1400             | .186              | .102  | .288  | .055         |

\* Pigment batch A-322

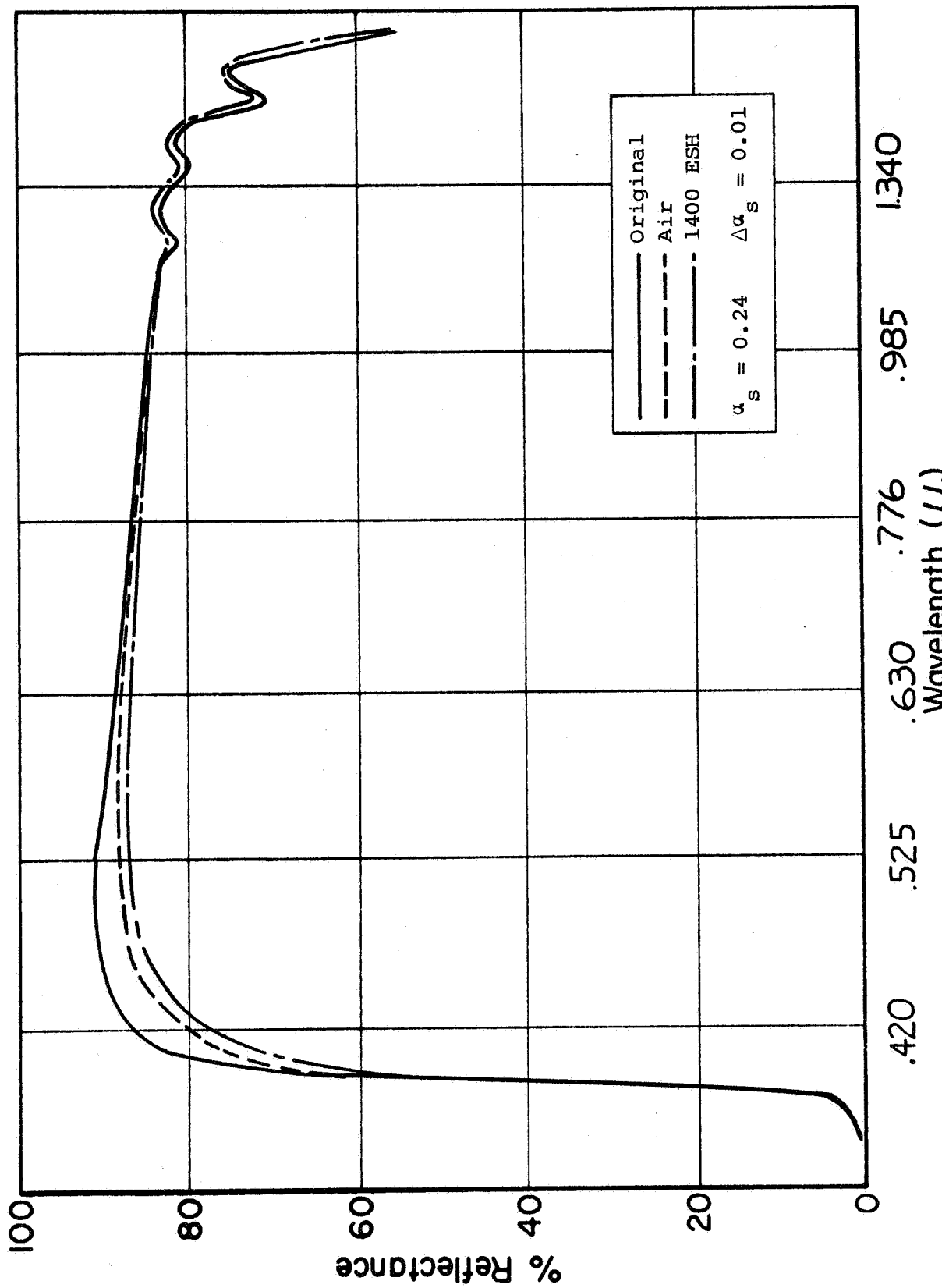


Fig. 22: EFFECT OF UV IRRADIATION IN THE IRIF ON S-13G PREPARED FROM SIFTED PIGMENT (PAINT GRIND TIME = 3 hr)

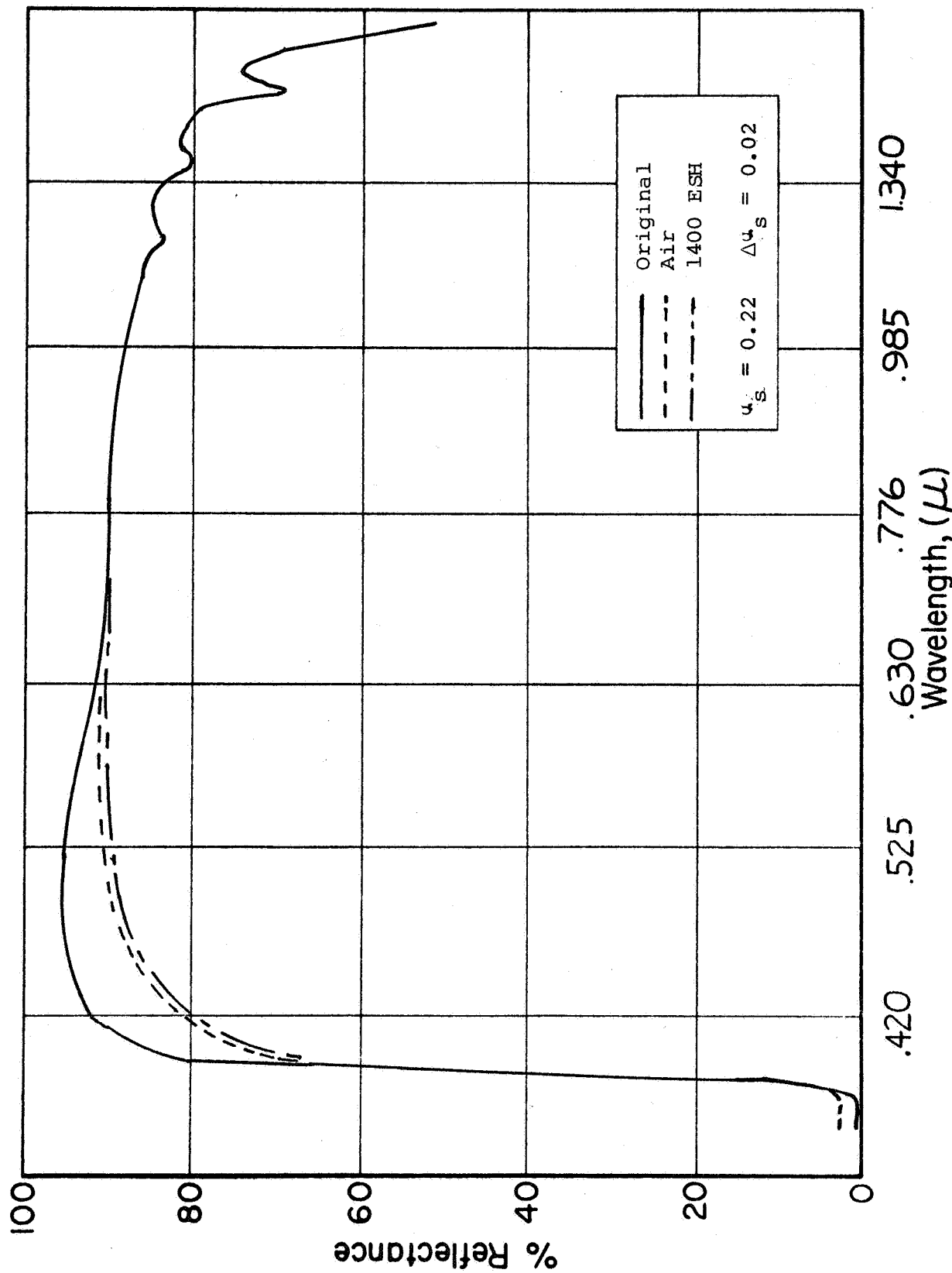


Fig. 23: EFFECT OF UV IRRADIATION IN THE IRIF ON S-13G PREPARED FROM UNSIFTED, UNGROUND PIGMENT (PAINT GRIND TIME = 4 hr)

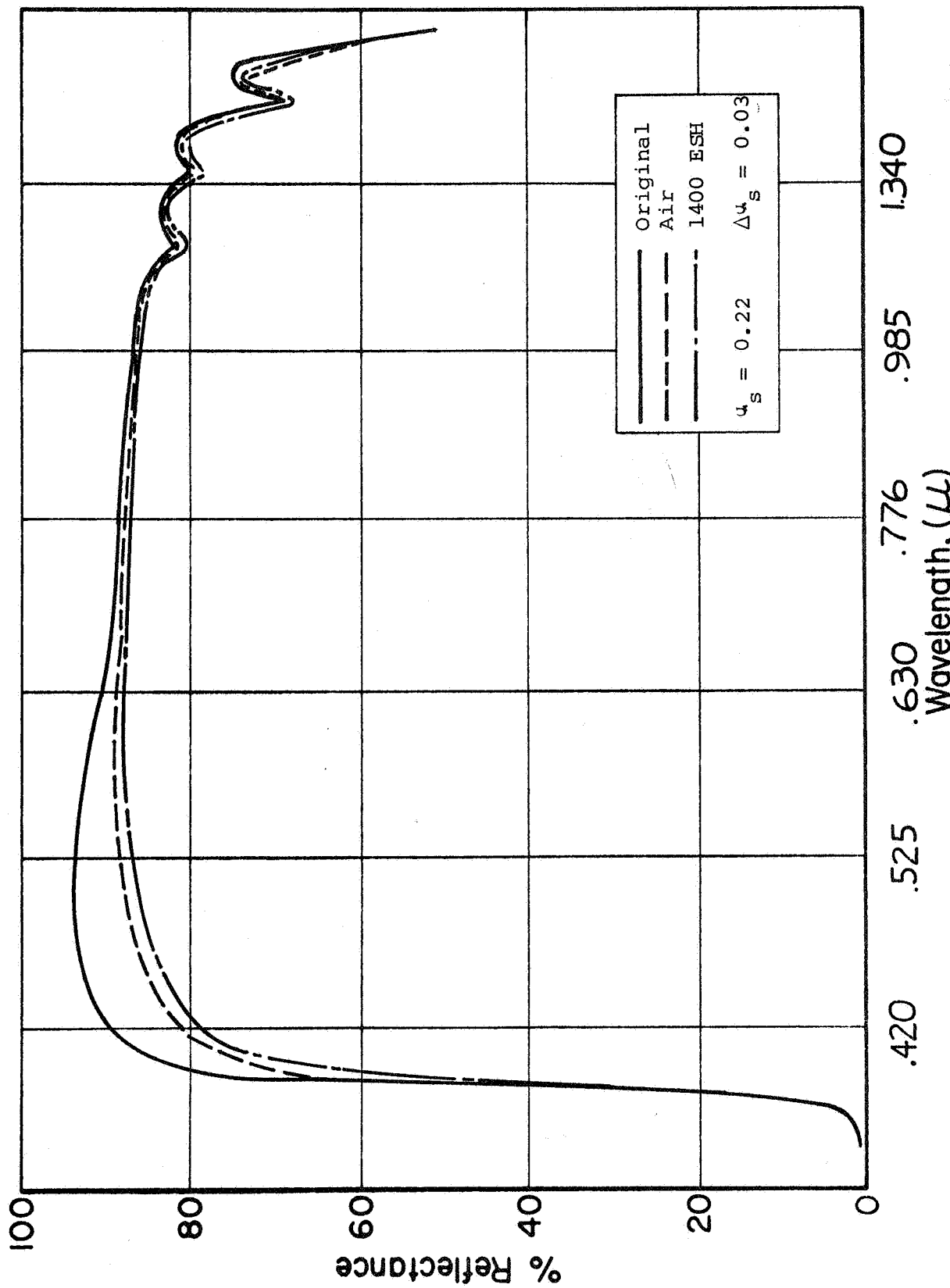


Fig. 24: EFFECT OF UV IRRADIATION IN THE IRIF ON S-13G PREPARED FROM DRY-GROUND (30 min) PIGMENT (PAINT GRIND TIME = 3 hr)



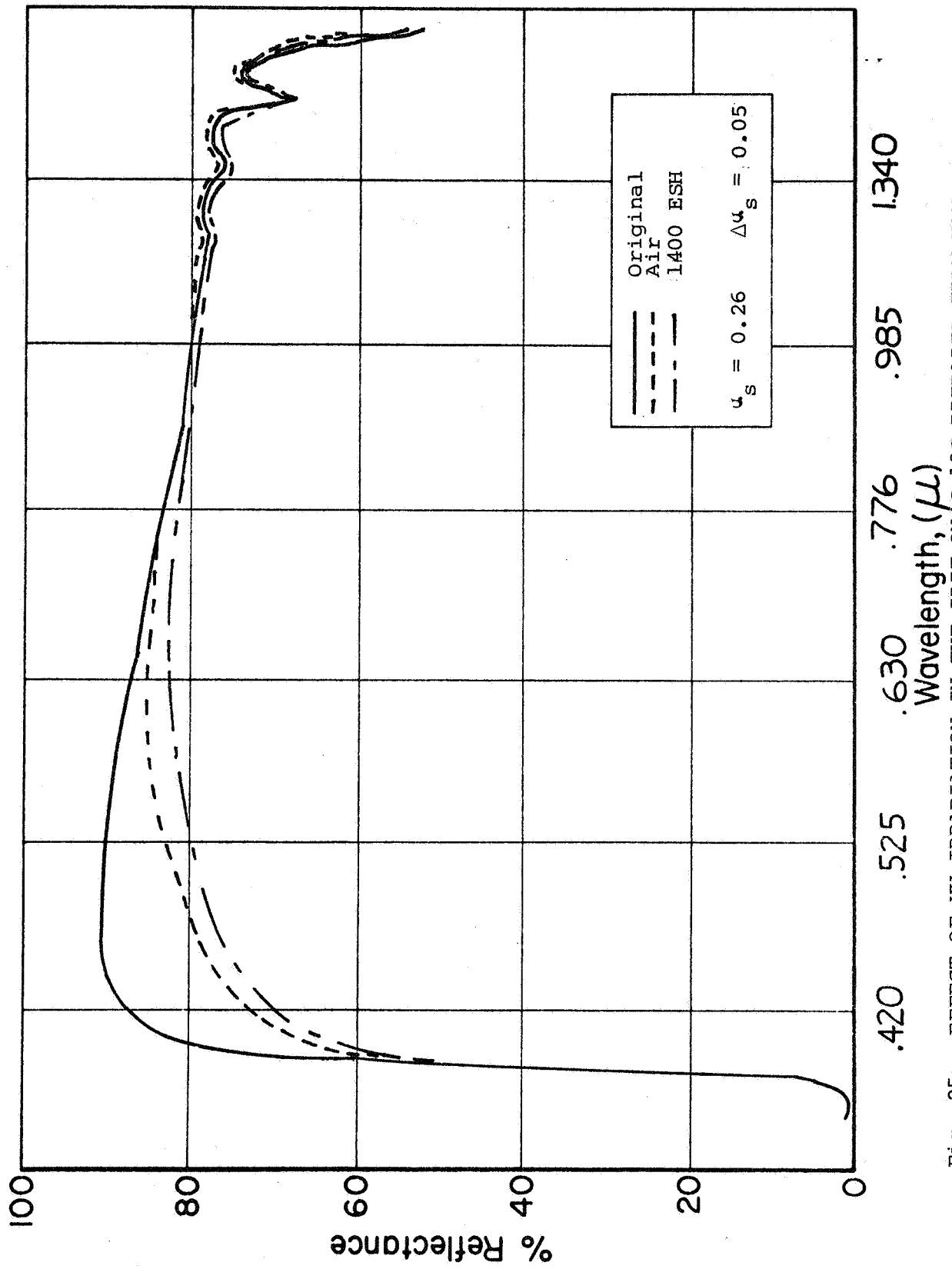


Fig. 25: EFFECT OF UV IRRADIATION IN THE IRIF ON S-13G PREPARED FROM HAND-MULLED PIGMENT (PAINT GRIND TIME = 3 hr)

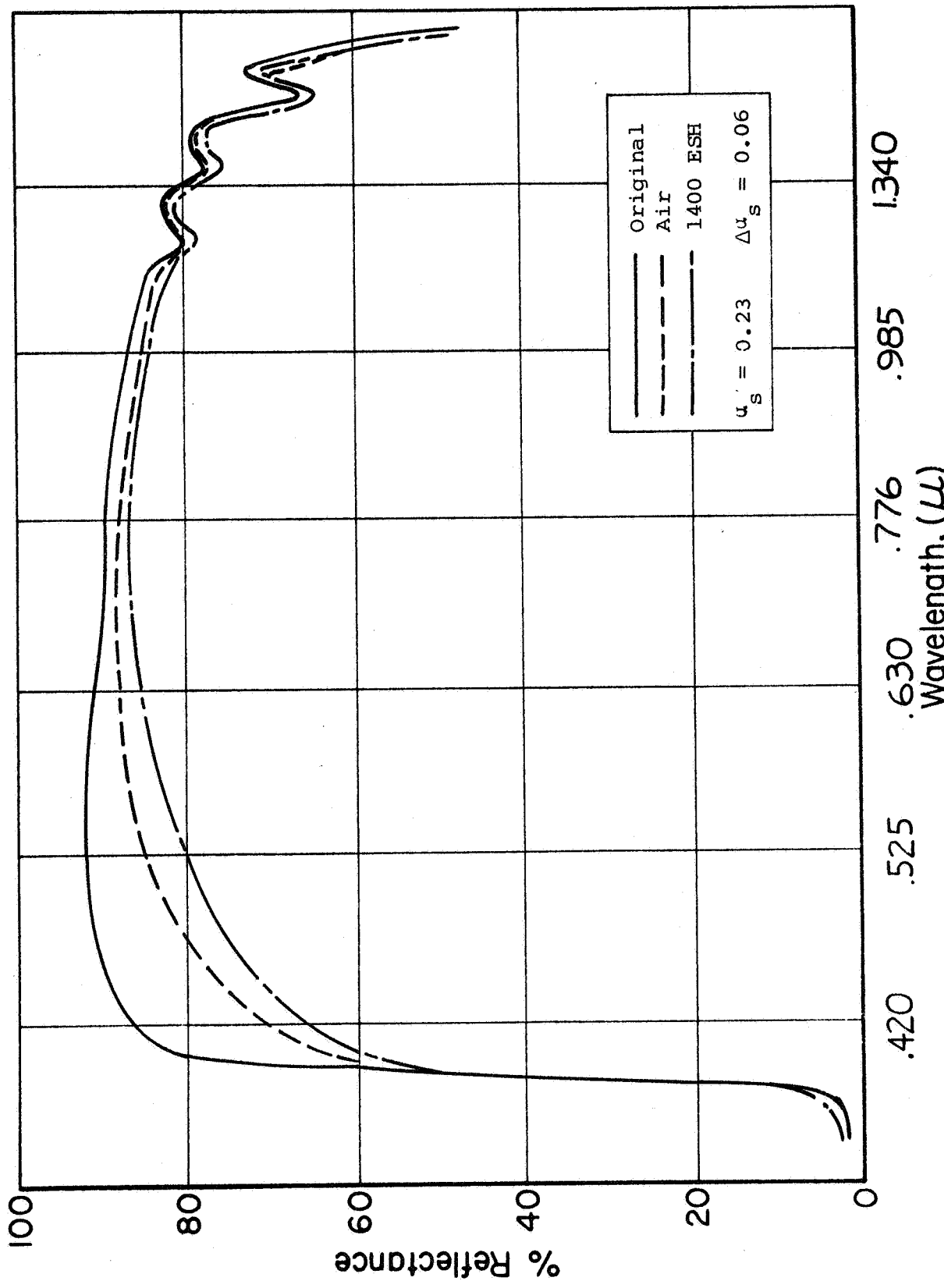


Fig. 26: EFFECT OF UV IRRADIATION IN THE IRIF ON S-13G PREPARED FROM REMULLED PIGMENT (PAINT GRIND TIME = 5 hr)

Hand-mulling procedures were employed in the manufacture of S-13G for the past 6 to 8 months, but this procedure was terminated as a result of these studies. Sifting out the millable pigment is a highly inefficient and costly technique, even though it permits shorter wet-grinding times and, therefore, greater stability; we therefore are presently wet-grinding only, but for a slightly longer period. Paint prepared from the pigment that was neither sifted nor dry-ground (or mulled) exhibited a  $\Delta u_s$  of 0.02 in 1400 ESH compared with 0.01 for the specimen prepared from pigment that was sifted (see Figures 22 and 23).

A specimen prepared from pigment that was first dry-ground for 30 min and subsequently wet ground for a short period exhibited a  $\Delta u_s$  of 0.03 in 1400 ESH.

Specimen 9 (Figure 26) was prepared by remulling the ends (too large to pass the sieve) from the first hand-mulling operation. Paint prepared from this pigment exhibited a  $\Delta u_s$  of 0.06 in 1400 ESH.

## V. UV-VACUUM SPECTROSCOPY

### A. Introduction

Ultraviolet absorption spectroscopy provides the chemist with a useful tool for determining the behavior of materials to both ionizing and ultraviolet radiation. Its usefulness, however, depends to a great extent upon the techniques employed in obtaining spectra. That is, the peak wavelength (absorption

band maxima) assignments and the quantitative interpretation of damage spectra depend not only on the resolution of the instruments employed but also on the purity of the materials and such influencing factors as, for example, solvent effects, which are known to considerably displace maxima. Additional errors occur in preparing differential spectra obtained by the subtraction or comparison of one transmittance spectrum from another, i.e. the comparison of an undamaged, control spectra with that of a damage spectra.

Because of the importance of analytical differential ultraviolet spectroscopy as an investigative tool in research aimed at the explanation of the mechanisms of damage to polymeric paint-binder systems, we have designed and constructed a dual-beam vacuum irradiation chamber for the Bausch & Lomb Spectronic 505 ultraviolet spectrophotometer. This attachment, which is presently being mated to the spectrophotometer, will be used in conjunction with ESR and other studies, all of which are aimed at the development of white pigmented coatings of greater stability than those presently available.

The importance of determining the optical properties of irradiated materials in the vacuum environment in which they are irradiated (in situ) has been discussed in numerous communications relating to this program. In summary, the fact that both air and visible light can rapidly bleach out color centers in polymeric species made the requirement for in situ transmittance measurements mandatory.

IIT RESEARCH INSTITUTE

## B. General Requirements

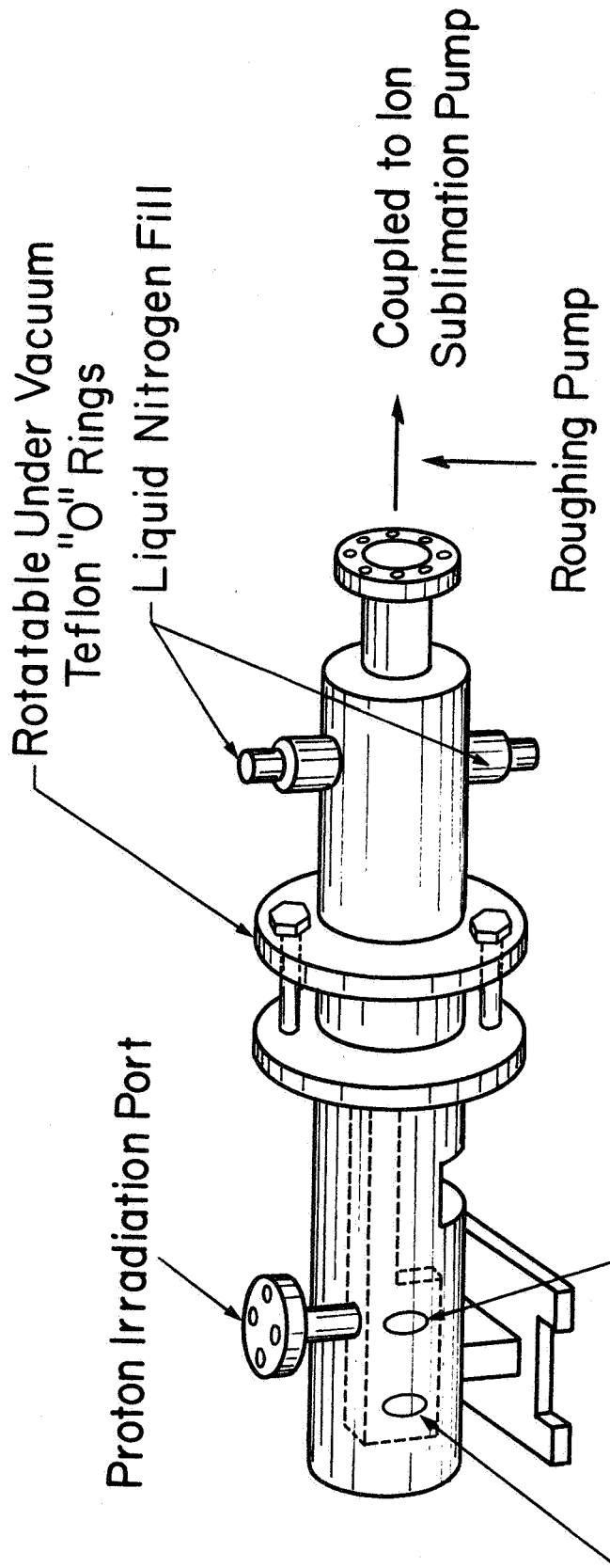
The general requirements for designing the dual-beam vacuum chamber were: (1) capability for determining in situ transmittance in the 200- to 700-m $\mu$  wavelength region, (2) that it be a modular attachment for the Bausch and Lomb Spectronic 505 spectrophotometer (although the concept can be adapted easily to the Cary or any other dual beam instrument), (3) capability of achieving a vacuum of  $1 \times 10^{-7}$  torr, (4) capability of irradiating the "sample" specimen with either ultraviolet or low-energy charged particles, and (5) temperature control of the sample mount by circulating liquid nitrogen, eutectic slushes, hot water, etc., through a reservoir.

The optical requirements of the attachment consist simply of the appropriate sapphire or fused silica ports for transmittance of the Spectronic 505's reference and sample beams.

A schematic of the dual-beam vacuum attachment is presented in Figure 27. This drawing shows the vacuum-irradiation chamber in which a rotatable (90°), temperature controlled sample-mounting table is located. The sample mounting table is a liquid reservoir that provides temperature control and is integral with the rotatable adaptor assembly to which the vacuum systems are attached.

The exterior sample and reference ports, as well as the rotatable specimen mounting ports, are separated by the exact dimension corresponding to the Spectronic 505's dual beams. They are positioned by a precision mount that "pins" the attachment into exact position in the sample compartment.

IIT RESEARCH INSTITUTE



Reference Saphire Measurement Ports      Sample      \* ROTATABLE FOR PROTON IRRADIATION AND TRANSMISSION MEASUREMENT

Fig. 27: SCHEMATIC OF DUAL-BEAM VACUUM CHAMBER

The sample specimen is irradiated through an off-center irradiation port (shown as the "proton irradiation port" in Figure 27); either ultraviolet (using a quartz window) or low energy charged particles can be employed. The specimen mount is maintained in a vertical position during transmission measurements and in a horizontal position during irradiation (rotated 90°). The reference sample is not irradiated and therefore provides the differential control during measurement.

The photograph in Figure 28 shows the vacuum-irradiation chamber with the specimen mount withdrawn (and in the vertical, measurement position). The specimen mount is shown in the irradiation position in Figure 29.

Figure 30 is a closeup photograph of the assembled unit. The mating flanges that contain the Teflon "o" ring are emphasized in this photograph. The complete assembly, showing the irradiation chamber attached to the Spectronic 505 and a 150 liter/sec ion/sublimation pump are shown in Figure 31.

#### D. Status

The system has been leak-tested and has achieved vacuums of  $3 \times 10^{-7}$  torr. The principle problem remaining is "shimming" the attachment's mount to the exact degree required to obtain optical alignment with the Spectronic 505. (The moment arm created by the attached ion pump has made precise positioning each time difficult).

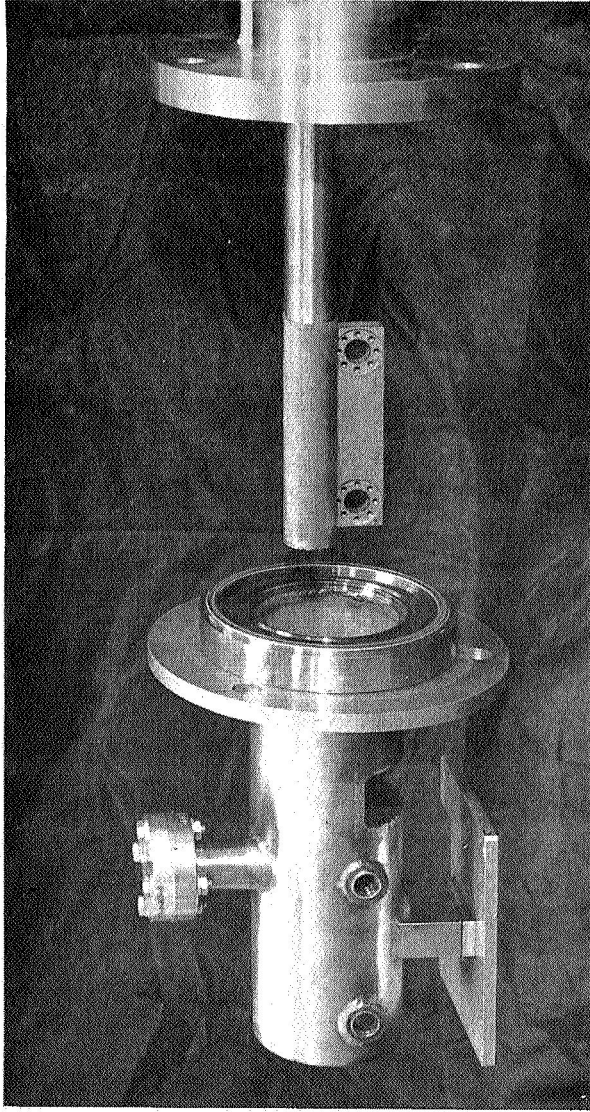


Fig. 28: THE IRRADIATION AND IN SITU MEASUREMENT CHAMBER (SAMPLE MOUNT IN MEASUREMENT POSITION)



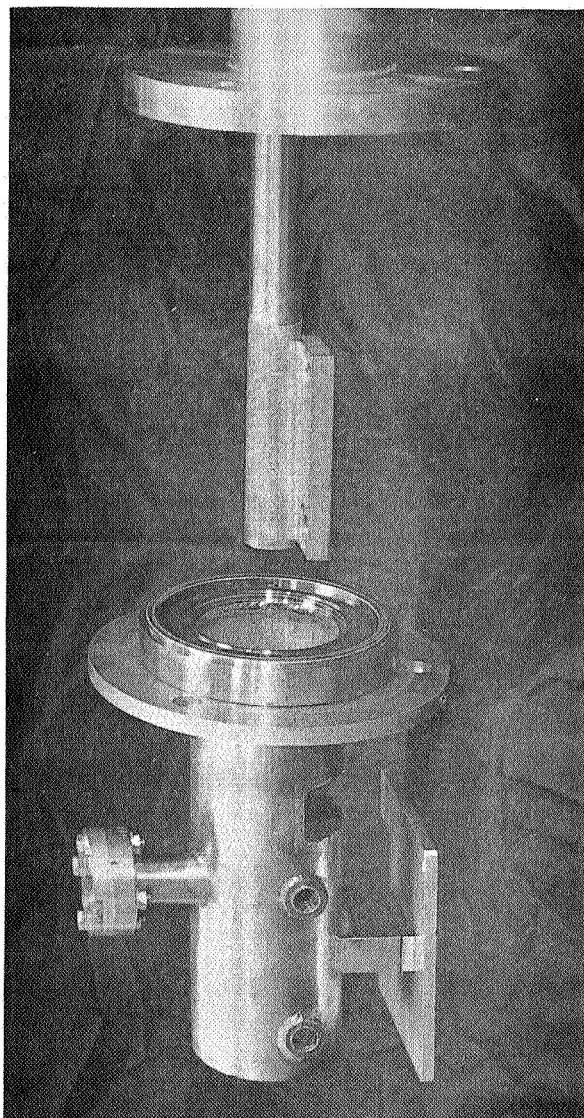


Fig 29: THE IRRADIATION AND IN SITU MEASUREMENT CHAMBER (SAMPLE MOUNT IN IRRADIATION POSITION)

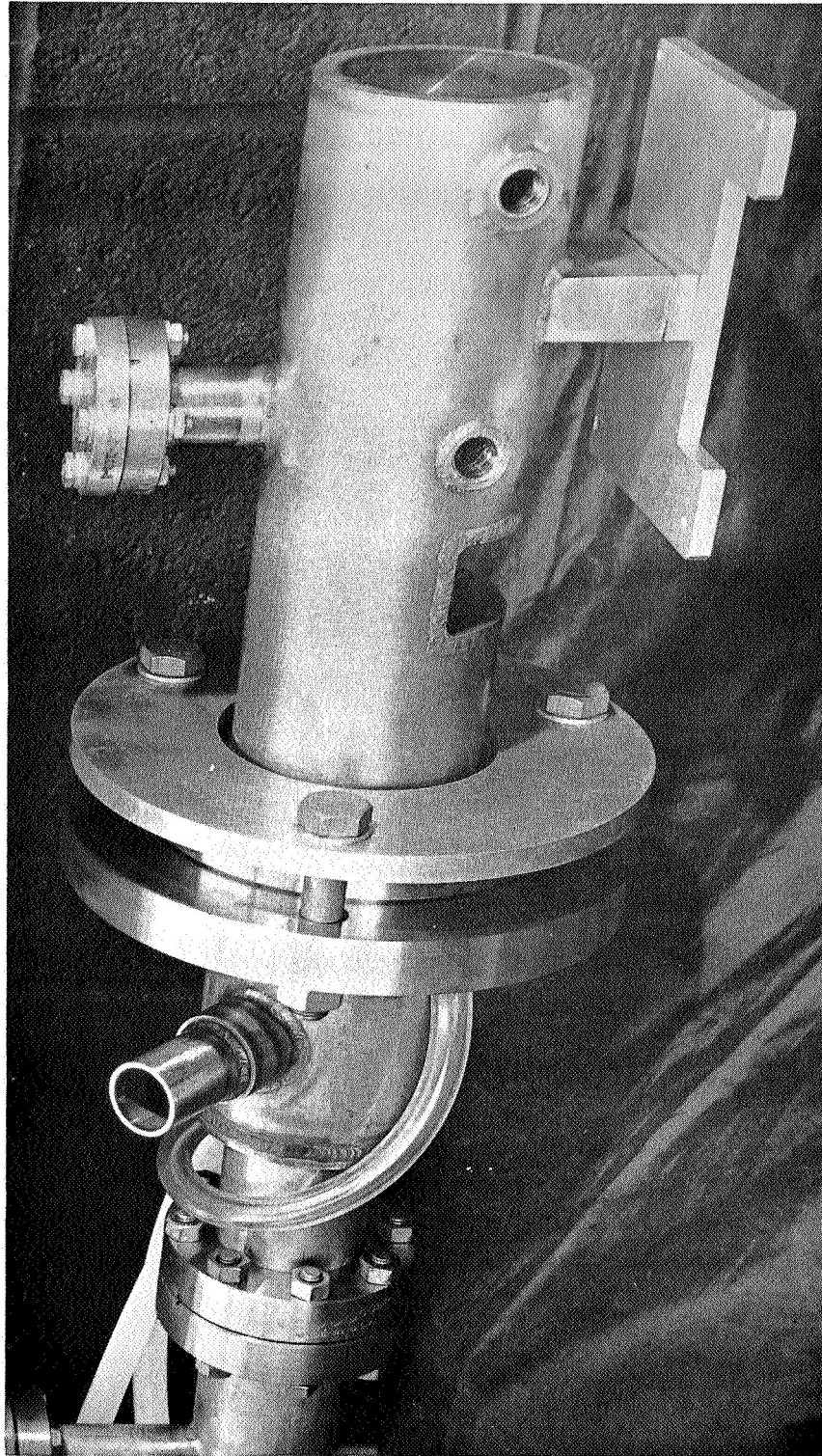


Fig. 30: CLOSE UP OF IRRADIATION CHAMBER SHOWING ROTATABLE "O" RING SEAL

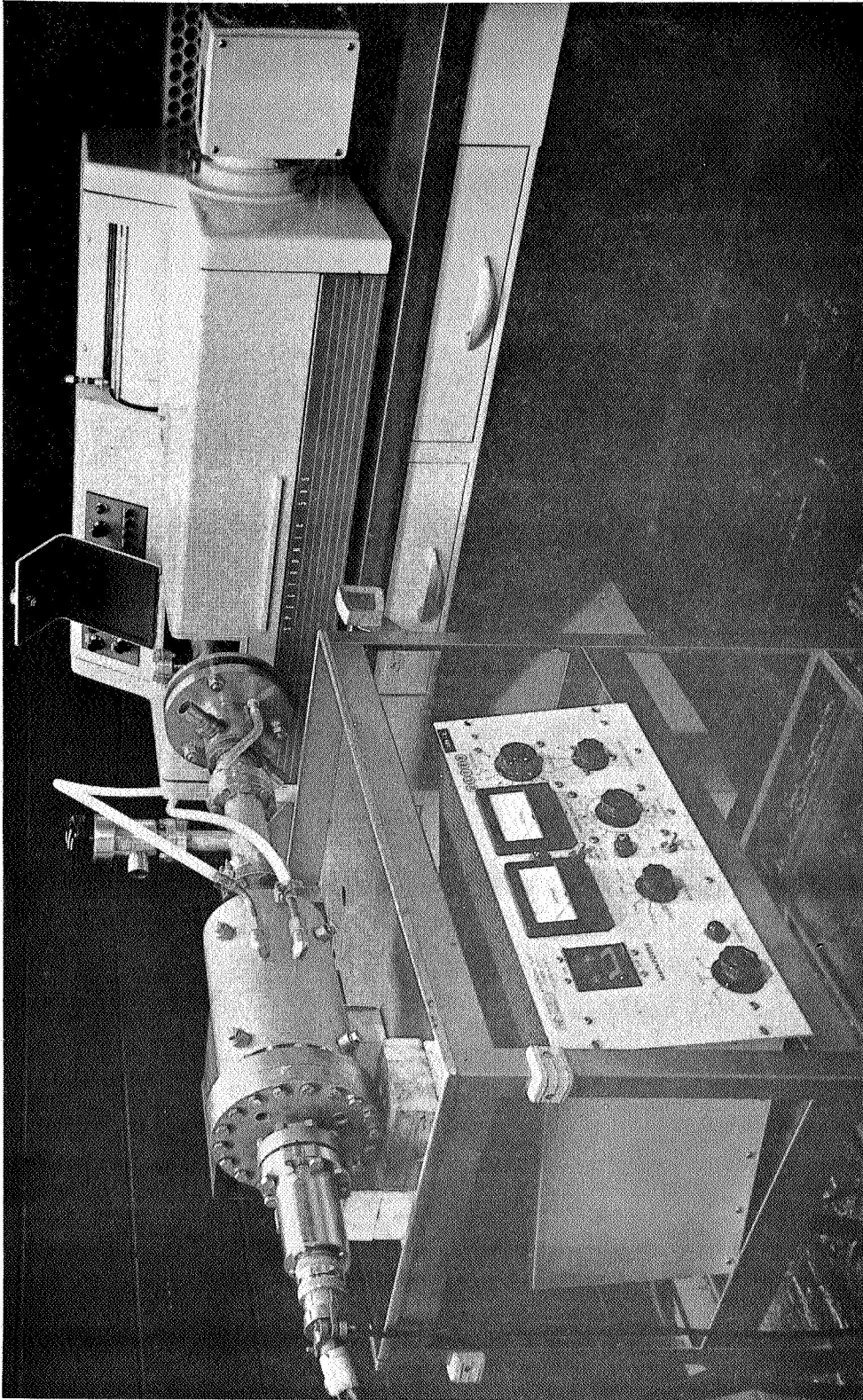


Fig. 31: THE DUAL-BEAM VACUUM CHAMBER MATED TO THE B&L SPECTRONIC 505 (SHOWING ATTACHED ION PUMP)

## VI. SUMMARY

Three zinc titanates have been synthesized; preliminary characterization studies have been performed. These titanates are:  $\text{ZnTiO}_3$ , the metatitanate;  $\text{Zn}_2\text{TiO}_4$ , the orthotitanate; and  $\text{Zn}_2\text{Ti}_3\text{O}_8$ , the sesquitanate. Of special significance is the correlation of their ultraviolet reflectance spectra with their stoichiometric composition. All three zinc titanates are prepared by firing intimate mixtures of the precursor oxides at temperatures of 700 to 1050°C.

Zinc orthotitanate,  $\text{Zn}_2\text{TiO}_4$ , is the whitest, most reflective and most stable of the three stoichiometries. The most stable product is formed at 1050°C. This product is extraordinarily hard and requires the expenditure of considerable energy to grind into a suitable powder. Indeed, it is believed that the requirement for grinding is largely responsible for the random instability that has been observed in space simulation tests employing in situ reflectance measurements (in the IRIF). That is, no attempt is made to eliminate the contribution of different particle-reduction (grinding) conditions from sample to sample and titanate to titanate. It is believed that severe particle reduction, such as is required to prepare samples of the orthotitanate fired at 1050°C, results in manifoldly increased instability as a consequence of a concomitant increase in the surface defect state. Zinc orthotitanate (and the metatitanate as well) exhibit bleachable degradation in the 0.4- to 1.5-  $\mu$  region, with the damage centered at about 0.9  $\mu$ .

IIT RESEARCH INSTITUTE



The extraction of all residual, unreacted zinc oxide with acetic acid has been found to be necessary for the elimination of strong absorption in zinc orthotitanate at 3500 A wavelength. Unextracted zinc oxide and excess titania are believed to be in part responsible for the bleachable infrared damage observed.

\* \* \* \* \*

The excellent stability of white vitreous porcelain enamels observed in earlier space simulation tests employing postexposure measurements in air was verified in a 1400-ESH in situ test in the IRIF. The initial solar absorptance of 0.31, which was not optimized (an old, random lab specimen of rutile-opacified borosilicate glass was used), was increased by only 0.007 in the 1400-ESH test.

\* \* \* \* \*

The importance of physical strain during grinding of pigmentary materials was emphasized by studies on the effect of grinding the potassium silicate-treated zinc oxide employed in IITRI's S-13G thermal-control coating. An S-13G specimen employing a sifted pigment that was not dry-ground prior to a 3-hr paint-grinding operation exhibited an increase in solar absorptance of 0.01 in 1400 ESH of irradiation in the IRIF. A specimen employing pigment that was first hand mulled and then wet-ground for 3 hr exhibited a  $\Delta u_s$  of 0.05; a specimen prepared from hand-mulled pigment that was wet-ground 5½ hr exhibited a  $\Delta u_s$  of 0.06 in 1400 ESH. Since sifting as a method of ensuring

IIT RESEARCH INSTITUTE

sufficiently deagglomerated particles is highly inefficient, a compromise method (one currently employed) consisted of wet grinding unsifted, unground silicate-treated pigment for 7 hr in the RTV-602 vehicle. This procedure resulted in an S-13G coating that exhibited a  $\Delta\alpha_s$  of 0.02 in the 1400 ESH test. We have found that 4-5 hrs of grinding is usually required to produce a satisfactory coating.

#### REFERENCES

1. Zerlaut, G. A., Harada, Y., and Tompkins, E. H., "Ultraviolet Irradiation of White Spacecraft Coatings in Vacuum," in Symposium on Thermal Radiation of Solids, S. Katzoff, ed., NASA SP-55, Washington, D.C., 1965.
2. Streed, E. R. and Beveridge, C. M., "The Study of Low Solar Absorptance Coatings for a Solar Probe," in Symposium on Thermal Radiation of Solids, S. Katzoff, ed., NASA SP-55, Washington, D.C., 1965.
3. Zerlaut, G. A., Gilligan, J. E., and Harada, Y., "Stable White Coatings," Report No. IITRI-C6027-16 (Interim Technical Progress Report), JPL Contract 950746 (subcontract under NAS7-100) conducted by IIT Research Institute, Chicago, Illinois, June 30, 1965.
4. Pearson, B. Douglas Jr., "Preliminary Results from the Ames Emissivity Experiment on OSO-II," in Progress in Astronautics and Aeronautics, G. Heller, ed., Vol. 18, Academic Press, N. Y., 1966, pp. 459-472.
5. Schafer, C. F. and Bannister, T. C., "Pegasus Thermal Control Coatings Experiment," AIAA 66-419, Los Angeles, June 27, 1966.
6. MacMillan, H. F., Sklensky, A. F., and McKellar, L. A., "Apparatus for Spectral Bidirectional Reflectance Measurements during Ultraviolet Irradiation in Vacuum," in Progress in Astronautics and Aeronautics, G. Heller, ed., Vol. 18, Academic Press, N. Y., 1966, pp. 129-149.
7. Miller, Edgar, NASA-George C. Marshall Space Flight Center, Huntsville, Alabama, personal communication, December 1965.
8. Zerlaut, G. A. and Rubin, G. A., "Development of Space-Stable Thermal-Control Coatings," Report No. IITRI-U6002-36 (Triannual Report), NASA-Marshall Space Flight Center, Contract NAS8-5379 conducted by IIT Research Institute, Chicago, Illinois, February 21, 1966.
9. Reference 8, Report IITRI-U6002-42, July 11, 1966.
10. Zerlaut, G. A. and Courtney, W. J., "Space-Simulation Facility for In Situ Reflectance Measurements," AIAA 67-312, New Orleans, La., April 19, 1967.

11. Edwards, D. K., Gier, J. T., Nelson, R., and Roddick, R. D., J. Opt. Soc. Am. 51, 1279 (1961).
12. Zerlaut, G. A. and Rogers, F. O., Reference 8, Report IITRI-U6002-47, November 30, 1966.
13. Bartram, S. F. and Slepety's, R. A., J. Am. Ceram. Soc. 44, 493-499 (1961).
14. Loskarev, B. A., Steklo i Keram. 19, No. 3, 22-66 (1962).
15. Loshkarev, B. A., Steklo i Keram. 19, No. 10, 21-24 (1962).
16. Loshkarev, B. A., Trans. Uralsk Polyteck. Inst. Symp. 117, 1962.
17. Kubo, T., Kato, M., et al, Kogyo Kagaku Zasshi 66, No. 4, 403-407 (1963).
18. Reference 8, Report IITRI-U6002-51, Feb. 28, 1967.
19. Lunsford, J. H., and Jayne, J. P., J. Chem. Phys. 44, 1487 (1966).
20. Collins, R. J., and Thomas, D. G., Phys. Rev. 112, 388 (1958).
21. Gilligan, J. E., "The Induced Optical Properties of Zinc Oxide," AIAA 67-214, New York, January 26, 1967.



DISTRIBUTION LIST

This report is being distributed as follows:

| <u>Copy No.</u>        | <u>Recipient</u>  |
|------------------------|---|
| 1-75 +<br>Reproducible | National Aeronautics & Space Administration<br>George C. Marshall Space Flight Center<br>Huntsville, Alabama<br>Attn: Mr. D. W. Gates (M-RP-T)                    |
| 76                     | National Aeronautics & Space Administration<br>George C. Marshall Space Flight Center<br>Huntsville, Alabama<br>Attn: PR-SC                                       |
| 77                     | National Aeronautics & Space Administration<br>George C. Marshall Space Flight Center<br>Huntsville, Alabama<br>Attn: MS-IL                                       |
| 78                     | National Aeronautics & Space Administration<br>George C. Marshall Space Flight Center<br>Huntsville, Alabama<br>Attn: MS-T  |
| 79-80                  | National Aeronautics & Space Administration<br>George C. Marshall Space Flight Center<br>Huntsville, Alabama<br>Attn: MS-I  |
| 81                     | Jet Propulsion Laboratory<br>California Institute of Technology<br>4800 Oak Grove Drive<br>Pasadena, California<br>Attn: Mr. W. F. Carroll                        |
| 82                     | National Aeronautics & Space Administration<br>Ames Research Center<br>Vehicle Systems Design Branch<br>Moffett Field, California 94035<br>Attn: Mr. E. R. Streed |
| 83                     | National Aeronautics & Space Administration<br>Office of Advanced Research & Technology<br>Washington, D. C.<br>Attn: Mr. Conrad Mook<br>Code RV                  |

IIT RESEARCH INSTITUTE

DISTRIBUTION LIST (CONT.)

| <u>Copy No.</u> | <u>Recipient</u>  |
|-----------------|---|
| 84              | IIT Research Institute<br>Division C Files                |
| 85              | IIT Research Institute<br>Editors, M. J. Klein/Main Files |
| 86              | IIT Research Institute<br>T. H. Meltzer, Division C       |
| 87              | IIT Research Institute<br>G. Noble, Division C            |
| 88              | IIT Research Institute<br>F. O. Rogers, Division C        |
| 89              | IIT Research Institute<br>G. Kimura, Division C           |
| 90              | IIT Research Institute<br>S. Shelfo, Division C           |
| 91              | IIT Research Institute<br>H. DeYoung, Division C          |
| 92              | IIT Research Institute<br>C. Donati, Division C           |
| 93              | IIT Research Institute<br>Y. Harada, Division G           |
| 94              | IIT Research Institute<br>W. J. Courtney, Division K      |

IIT RESEARCH INSTITUTE